Transverse Centroid and Envelope Descriptions of Beam Evolution*

Steven M. Lund
Lawrence Livermore National Laboratory (LLNL)

Steven M. Lund and John J. Barnard
"Beam Physics with Intense Space-Charge"
US Particle Accelerator School
Boston University, Waltham, MA
12-23 June, 2006

* Research supported by the US Dept. of Energy at LBNL and LLNL under contract Nos. DE-AC03-76SF00098 and W-7405-Eng-48

Transverse Centroid and Envelope Model: Outline

Comments:

- Some of this material related to J.J. Barnard lectures:
  - Transport limit discussions (Introduction)
  - Transverse envelope modes (Cont. Focusing Envelope Modes and Halo)
  - Longitudinal envelope evolution (Longitudinal Beam Physics III)
  - 3D Envelope Modes in a Bunched Beam (Cont. Focusing Envelope Modes and Halo)
- Specific topics will be covered in more detail here

Transverse Centroid and Envelope Model: Detailed Outline

Detailed Outline - 2

S1: Overview

Analyze transverse centroid and envelope properties of an unbunched $(\partial/\partial z = 0)$ beam

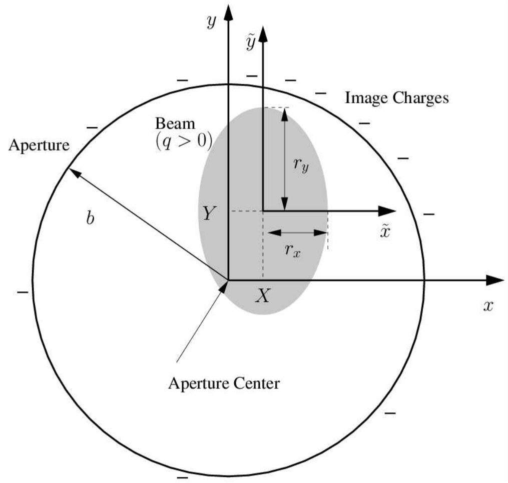

Centroid:

$$\boxed{\begin{aligned} X &= \langle x \rangle_\perp \\ Y &= \langle y \rangle_\perp \end{aligned}}$$

x- and y-coordinates of beam center of mass

$$\langle \cdots \rangle_\perp \equiv \frac{\int d^2x_\perp \int d^2x'_\perp \ \cdots f_\perp}{\int d^2x_\perp \int d^2x'_\perp \ f_\perp}$$

Envelope:

$$\boxed{\begin{aligned} r_x &= 2\sqrt{\langle (x-X)^2 \rangle_\perp} \\ r_y &= 2\sqrt{\langle (y-Y)^2 \rangle_\perp} \end{aligned}}$$

x- and y-principal axis radii of an elliptical beam envelope

Oscillations in the statistical beam centroid and envelope radii are the *lowest-order* collective responses of the beam

Centroid Oscillations: Associated with errors and are purposefully suppressed to the level possible

- Error Sources:
  - Beam distribution
  - Dipole bending terms from applied field optics
  - Imperfect mechanical alignment
- Exception: When the beam is kicked (insertion or extraction) into our out of a transport channel as is often done in rings

Envelope Oscillations: Can have two components in periodic lattices

Matched Envelope: Periodic flutter synchronized to periodic focusing structure to produce net focusing

Mismatched Envelope: Excursions deviate from matched flutter motion and are seeded/driven by errors

Maximum radial confinement of the maximum beam-edge excursions are desired for economical transport

- Reduces cost by Limiting material volume needed to transport an intense beam

Mismatched beams have larger envelope excursions and have more stability problems since mismatch adds another source of free energy that can drive statistical increases in particle amplitudes (Halo, see J.J. Barnard Lectures on Halo)

Example: FODO Quadrupole Transport Channel

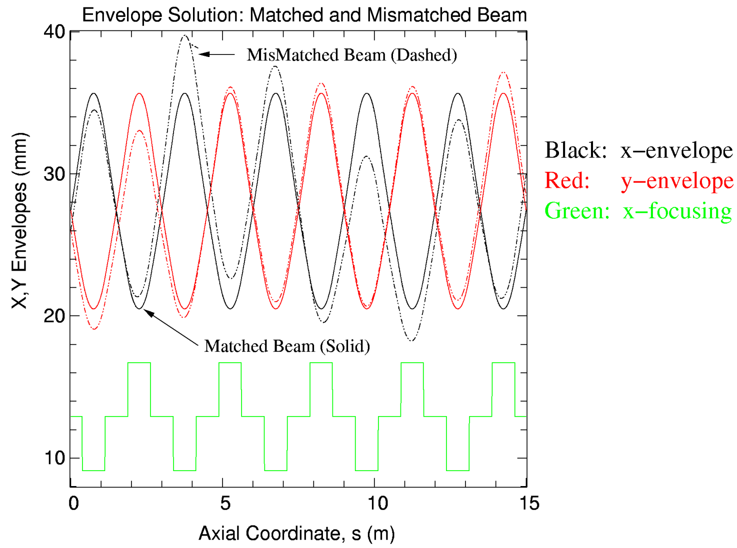

- Larger machine aperture is needed to confine a mismatched beam

Centroid and Envelope oscillations are the *most important collective modes* of an intense beam

- Force balances based on matched beam envelope equation predict scaling of transportable beam parameters
  - Used to design transport lattices
- Instabilities in beam centroid and/or envelope oscillations prevent reliable transport
  - Parameter locations of instability regions should be understood and avoided in machine design

Although it is *necessary* to design to avoid envelope and centroid instabilities, it is not alone *sufficient* for effective machine operation

- Higher-order kinetic and fluid instabilities not expressed in the low-order envelope models can degrade beam quality and control and must also be evaluated
  - To be covered (see S.M. Lund, lectures on *Kinetic Stability*)

S2: Derivation of Transverse Centroid and Envelope Equations of Motion

Analyze centroid and envelope properties of an unbunched $(\partial/\partial z = 0)$ beam

Transverse Statistical Averages:

Let N be the number of particles in a thin axial slice of the beam at axial coordinate s.

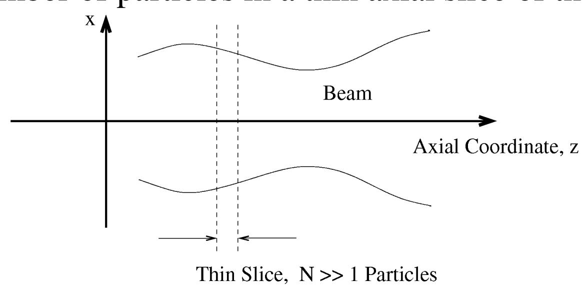

Equivalent averages can be defined in terms of the particles or the transverse Vlasov distribution function:

particles: $$\langle \cdots \rangle_\perp \equiv \frac{1}{N}\sum_{i=1}^{N} \cdots$$

distribution: $$\langle \cdots \rangle_\perp \equiv \frac{\int d^2x_\perp \int d^2x'_\perp \ \cdots f_\perp}{\int d^2x_\perp \int d^2x'_\perp \ f_\perp}$$

- Averages can be generalized to include axial momentum spread

Transverse Particle Equations of Motion

Consistent with earlier analysis, take:

$$x'' + \frac{(\gamma_b\beta_b)'}{(\gamma_b\beta_b)}x' + \kappa_x x = -\frac{q}{m\gamma_b^3\beta_b^2c^2}\frac{\partial\phi}{\partial x}$$

$$y'' + \frac{(\gamma_b\beta_b)'}{(\gamma_b\beta_b)}y' + \kappa_y y = -\frac{q}{m\gamma_b^3\beta_b^2c^2}\frac{\partial\phi}{\partial y}$$

$$\nabla_\perp^2\phi = \left(\frac{\partial^2}{\partial x^2} + \frac{\partial^2}{\partial y^2}\right)\phi = -\frac{\rho}{\epsilon_0}$$

$$\phi|_{\text{aperture}} = 0$$

Assume:
- Unbunched beam
- No axial momentum spread
- Linear applied focusing fields
- Possible acceleration

Various apertures are possible. Some simple examples:

Round Pipe

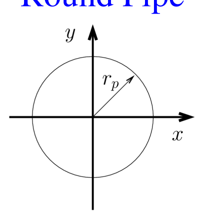

Linac magnetic quadrupoles, acceleration cells, ...

Elliptical Pipe

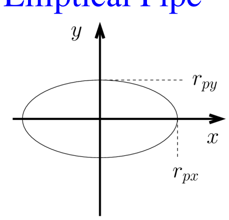

Dispersive rings in drifts, magnetic optics, ...

Hyperbolic Sections

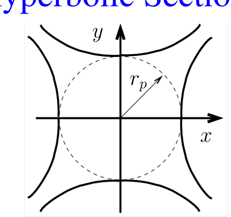

Electric quadrupoles

Review: Focusing lattices we will take in examples: Continuous and piecewise constant periodic solenoid and quadrupole doublet

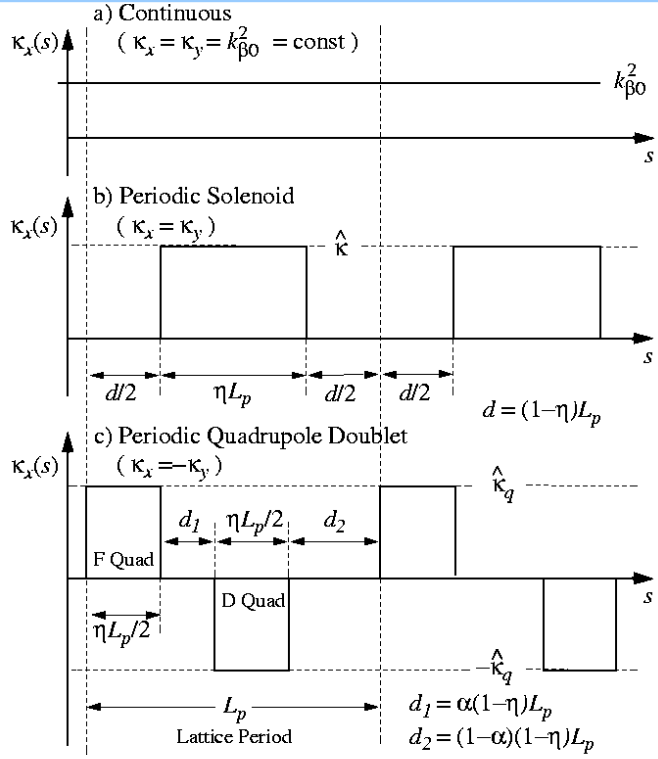

Lattice Period L_p

Occupancy η

$\eta \in [0, 1]$

Solenoid description carried out implicitly in Larmor frame

[see Lund and Bukh, PRST- Accel. and Beams 7, 024801 (2004), Appendix A]

Syncopation Factor α

$$\alpha \in [0, \frac{1}{2}]$$

$$\alpha = \frac{1}{2} \implies FODO$$

Distribution Assumptions

To lowest order, linearly focused intense beams are expected to be nearly uniform in density within the core of the beam out to an edge where the density falls rapidly to zero

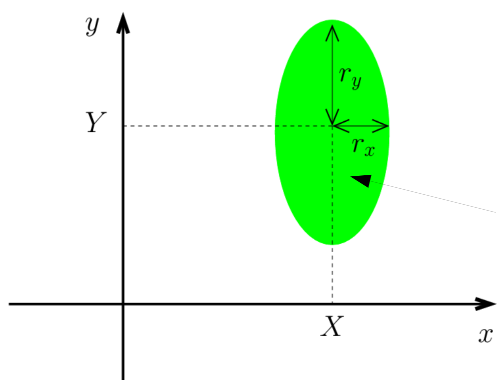

constant density in the beam:

$$\rho = \frac{\lambda}{\pi r_x r_y} = \text{const}$$

$$\rho(x,y) = q \int d^2x'_\perp \, f_\perp \simeq \begin{cases} \frac{\lambda}{\pi r_x r_y}, & (x-X)^2/r_x^2 + (y-Y)^2/r_y^2 < 1 \\ 0, & (x-X)^2/r_x^2 + (y-Y)^2/r_y^2 > 1 \end{cases}$$

$$\lambda = q \int d^2x_\perp \int d^2x'_\perp \, f_\perp = \int d^2x \, \rho$$

Self-Field Calculation

Temporarily, we will consider an arbitrary beam charge distribution within an arbitrary aperture to formulate the problem.

Electrostatic field of a line charge in free-space

$$\boxed{\mathbf{E}_\perp = \frac{\lambda_0}{2\pi\epsilon_0}\frac{(\mathbf{x}_\perp - \tilde{\mathbf{x}})}{|\mathbf{x}_\perp - \tilde{\mathbf{x}}|^2}}$$

$\lambda_0 =$ line charge

$\mathbf{x}_\perp = \tilde{\mathbf{x}} =$ coordinate of charge

Resolve the field of the beam into direct (free space) and image terms:

$$\boxed{\mathbf{E}^s_\perp = -\frac{\partial\phi}{\partial\mathbf{x}_\perp} = \mathbf{E}^d_\perp + \mathbf{E}^i_\perp}$$

and superimpose free-space solutions for direct and image contributions

Direct Field

$$\mathbf{E}^d_\perp(\mathbf{x}_\perp) = \frac{1}{2\pi\epsilon_0}\int d^2\tilde{x}_\perp \, \frac{\rho(\tilde{\mathbf{x}}_\perp)(\mathbf{x}_\perp - \tilde{\mathbf{x}}_\perp)}{|\mathbf{x}_\perp - \tilde{\mathbf{x}}_\perp|^2}$$

$\rho(\mathbf{x}) =$ beam charge density

Image Field

$$\mathbf{E}^i_\perp(\mathbf{x}_\perp) = \frac{1}{2\pi\epsilon_0}\int d^2\tilde{x}_\perp \, \frac{\rho^i(\tilde{\mathbf{x}}_\perp)(\mathbf{x}_\perp - \tilde{\mathbf{x}}_\perp)}{|\mathbf{x}_\perp - \tilde{\mathbf{x}}_\perp|^2}$$

$\rho^i(\mathbf{x}) =$ beam image charge density

Direct Field:

For a uniform density elliptical beam the direct contribution is as calculated for the KV equilibrium, free-space self-field calculation

- see S.M. Lund lectures on *Transverse Beam Equilibria*

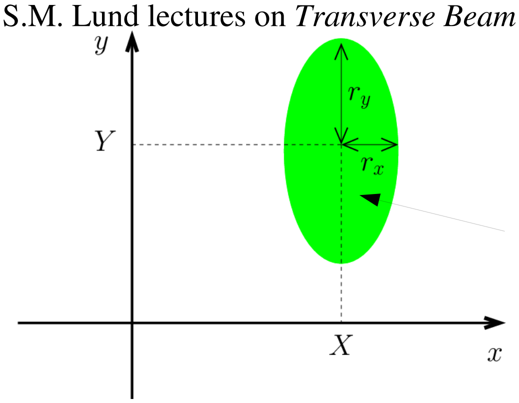

constant density in the beam:

$$\rho = \frac{\lambda}{\pi r_x r_y} = \text{const}$$

$$\boxed{\begin{aligned} E^d_x &= \frac{\lambda}{\pi\epsilon_0}\frac{x - X}{(r_x + r_y)r_x} \\ E^d_y &= \frac{\lambda}{\pi\epsilon_0}\frac{y - Y}{(r_x + r_y)r_y} \end{aligned}}$$

Image Field:

Image structure depends on the aperture. Assume a round pipe for simplicity.

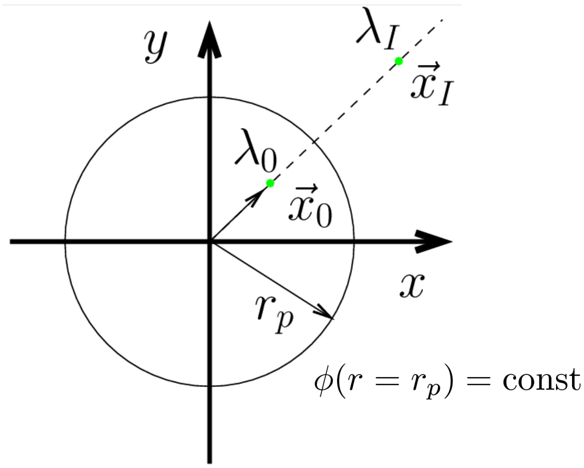

$\lambda_I = -\lambda_0$ image charge

$\mathbf{x}_I = \frac{r_p^2}{|\mathbf{x}_0|^2}\mathbf{x}_0$ image location

superimpose all images of beam:

$$\boxed{\mathbf{E}^i_\perp(\mathbf{x}_\perp) = -\frac{1}{2\pi\epsilon_0}\int_{\text{pipe}} d^2\tilde{x}_\perp \, \frac{\rho(\tilde{\mathbf{x}}_\perp)(\mathbf{x}_\perp - r_p^2\tilde{\mathbf{x}}_\perp/|\tilde{\mathbf{x}}_\perp|^2)}{|\mathbf{x}_\perp - r_p^2\tilde{\mathbf{x}}_\perp/|\tilde{\mathbf{x}}_\perp|^2|^2}}$$

- Difficult to calculate even for a uniform density beam

Examine limits of the image field:

1) On-axis line charge: $\rho(\mathbf{x}_\perp) = \lambda\delta(\mathbf{x}_\perp - X\hat{\mathbf{e}}_x)$

$$\boxed{\mathbf{E}^i_\perp(\mathbf{x}_\perp = X\mathbf{e}_x) = \frac{\lambda}{2\pi\epsilon_0(r_p^2/X - X)}\hat{\mathbf{e}}_x}$$

- Generates nonlinear field at position of direct charge

2) Centered, uniform density elliptical beam:

Expand using complex coordinates starting from the general image expression:

$$\underline{E}^i = E^i_y + iE^i_x = \sum_{n=2,4,\cdots}^{\infty} \underline{c}_n \underline{z}^{n-1} \qquad \underline{c}_n = \frac{i}{2\pi\epsilon_0}\int_{\text{pipe}} d^2x_\perp \, \rho(\mathbf{x}_\perp)\frac{(x-iy)^n}{r_p^{2n}}$$

$$\underline{z} = x + iy \qquad = \frac{i\lambda n!}{2\pi\epsilon_0 2^n (n/2+1)!(n/2)!}\left(\frac{r_x^2 - r_y^2}{r_p^4}\right)^{n/2}$$

$$i = \sqrt{-1}$$

The linear (n=2) components of this expansion give:

$$\boxed{E^i_x = \frac{\lambda}{8\pi\epsilon_0}\frac{r_x^2 - r_y^2}{r_p^4}x, \qquad E^i_y = -\frac{\lambda}{8\pi\epsilon_0}\frac{r_x^2 - r_y^2}{r_p^4}y}$$

- Rapidly vanish (higher order terms more rapid) as beam becomes more round

3) Elliptical beam with a small displacement along the x-axis:

$$Y = 0 \qquad |X|/r_p \ll 1$$

Expand using complex coordinates starting from the general image expression:

- Use complex coordinates to simplify calculation

  E.P. Lee, E. Close, and L. Smith, Nuc. Instr. Meth, 1126 (1987)
- Expressions become even more complicated with simultaneous x- and y-displacements and more complicated aperture geometries

$$E_x^i = \frac{\lambda}{2\pi\epsilon_0 r_p^2}\left[f(x-X) + gX\right] + \Theta\left(\frac{X}{r_p}\right)^3$$

$$E_y^i = -\frac{\lambda}{2\pi\epsilon_0 r_p^2} f y + \Theta\left(\frac{X}{r_p}\right)^3$$

$$f = \frac{r_x^2 - r_y^2}{4r_p^2} + \frac{X^2}{r_p^2}\left[1 + \frac{3}{2}\left(\frac{r_x^2 - r_y^2}{r_p^2}\right) + \frac{3}{8}\left(\frac{r_x^2 - r_y^2}{r_p^2}\right)^2\right]$$

$$g = 1 + \frac{r_x^2 - r_y^2}{4r_p^2} + \frac{X^2}{r_p^2}\left[1 + \frac{3}{4}\left(\frac{r_x^2 - r_y^2}{r_p^2}\right) + \frac{1}{8}\left(\frac{r_x^2 - r_y^2}{r_p^2}\right)^2\right]$$

Comments on images:

- Sign is generally such that it will tend to increase beam displacements
  - Also weaker focusing corrections for an elliptical beam
- Can be very difficult to calculate explicitly
  - Even for simple case of circular pipe
  - Special cases of simple geometry formulas can give idea on scaling
  - Generally suppress just by making the beam small relative to characteristic dimensions and keeping the beam near-axis
- Depend strongly on the aperture geometry
  - Generally varies as a function of s in the machine

Round Pipe

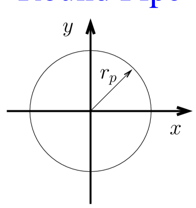

Elliptical Pipe

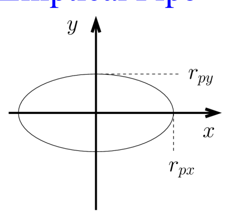

Hyperbolic Sections

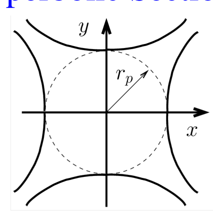

Coupled centroid and envelope equations of motion

Consistent with the assumed structure of the distribution (uniform density elliptical beam), denote:

Beam Centroid:

$$\boxed{\begin{aligned} X &\equiv \langle x \rangle_\perp \\ Y &\equiv \langle y \rangle_\perp \end{aligned}}$$

Coordinates with respect to centroid:

$$\boxed{\begin{aligned} \tilde{x} &\equiv x - X \\ \tilde{y} &\equiv y - Y \end{aligned}}$$

Envelope Edge Radii:

$$\boxed{\begin{aligned} r_x &= 2\sqrt{\langle \tilde{x}^2 \rangle_\perp} \\ r_y &= 2\sqrt{\langle \tilde{y}^2 \rangle_\perp} \end{aligned}}$$

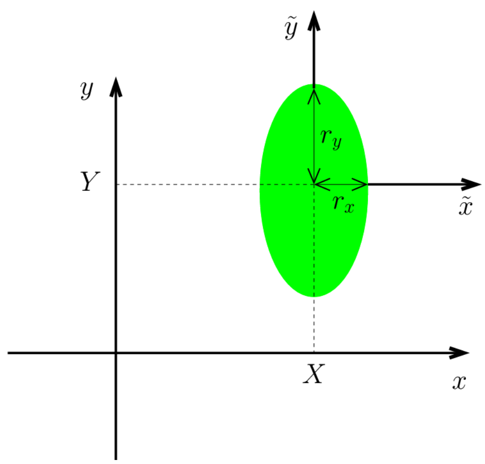

With the assumed uniform elliptical beam, all moments can be calculated in terms of: $X, \quad Y \qquad r_x, \quad r_y$

To derive centroid equations, first use the self-field resolution for a uniform density beam, then the equations of motion for a particle within the beam can be expressed as:

$$x'' + \frac{(\gamma_b\beta_b)'}{(\gamma_b\beta_b)}x' + \kappa_x x - \frac{2Q}{(r_x+r_y)r_x}(x-X) = \frac{q}{m\gamma_b^3\beta_b^2c^2}E_x^i$$

$$y'' + \frac{(\gamma_b\beta_b)'}{(\gamma_b\beta_b)}y' + \kappa_y y - \frac{2Q}{(r_x+r_y)r_y}(y-Y) = \frac{q}{m\gamma_b^3\beta_b^2c^2}E_y^i$$

Direct Terms Image Terms

perveance:

$$Q \equiv \frac{q\lambda}{2\pi\epsilon_0 m\gamma_b^3\beta_b^2c^2}$$

average equations using: $\langle x' \rangle_\perp = \langle x \rangle'_\perp = X'$ etc., to obtain:

Centroid Equations:

$$\boxed{\begin{aligned} X'' + \frac{(\gamma_b\beta_b)'}{(\gamma_b\beta_b)}X' + \kappa_x X &= Q\frac{2\pi\epsilon_0}{\lambda}\langle E_x^i \rangle_\perp \\ Y'' + \frac{(\gamma_b\beta_b)'}{(\gamma_b\beta_b)}Y' + \kappa_y Y &= Q\frac{2\pi\epsilon_0}{\lambda}\langle E_y^i \rangle_\perp \end{aligned}}$$

- $\langle E_x^i \rangle_\perp$ will generally depend on: $X, \quad Y$ and $r_x, \quad r_y$

To derive equations of motion for the envelope radii, first subtract the X centroid equation from the x-particle equation of motion to obtain:

$$\tilde{x} \equiv x - X$$

$$\tilde{x}'' + \frac{(\gamma_b\beta_b)'}{(\gamma_b\beta_b)}\tilde{x}' + \kappa_x\tilde{x} - \frac{2Q\tilde{x}}{(r_x+r_y)r_x} = \frac{q}{m\gamma_b^2\beta_b^2c^2}\left[E_x^i - \langle E_x^i\rangle_\perp\right]$$

Differentiate the equation for the envelope radius:

$$r_x = 2\langle\tilde{x}^2\rangle_\perp^{1/2} \longrightarrow r_x' = \frac{4\langle\tilde{x}\tilde{x}'\rangle_\perp}{r_x}$$

Define (motivated the KV equilibrium results) a statistical rms edge emittance:

$$\varepsilon_x \equiv 4\varepsilon_{x,\mathrm{rms}} = 4\left[\langle\tilde{x}^2\rangle_\perp\langle\tilde{x}'^2\rangle_\perp - \langle\tilde{x}\tilde{x}'\rangle_\perp^2\right]^{1/2}$$

Differentiate the equation for r_x' again and use the emittance definition:

$$r_x'' = 4\frac{\langle\tilde{x}\tilde{x}''\rangle_\perp}{r_x} + \frac{16[\langle\tilde{x}^2\rangle_\perp\langle\tilde{x}'^2\rangle_\perp - \langle\tilde{x}\tilde{x}'\rangle_\perp^2]}{r_x^3}$$

$$= 4\frac{\langle\tilde{x}\tilde{x}''\rangle_\perp}{r_x} + \frac{\varepsilon_x^2}{r_x^3}$$

and then employ the equations of motion to eliminate $\tilde{x}''$ in $\langle\tilde{x}\tilde{x}''\rangle_\perp$ to obtain:

Envelope Equations:

$$\boxed{\begin{aligned} r_x'' + \frac{(\gamma_b\beta_b)'}{(\gamma_b\beta_b)}r_x' + \kappa_x r_x - \frac{2Q}{r_x+r_y} - \frac{\varepsilon_x^2}{r_x^3} &= 4Q\frac{2\pi\epsilon_0}{\lambda}\langle\tilde{x}E_x^i\rangle_\perp \\ r_y'' + \frac{(\gamma_b\beta_b)'}{(\gamma_b\beta_b)}r_x' + \kappa_y r_y - \frac{2Q}{r_x+r_y} - \frac{\varepsilon_y^2}{r_y^3} &= 4Q\frac{2\pi\epsilon_0}{\lambda}\langle\tilde{x}E_x^i\rangle_\perp \end{aligned}}$$

- $\langle\tilde{x}E_x^i\rangle_\perp$ will generally depend on: X, Y and r_x, r_y

Comments on Centroid/Envelope equations:

- Centroid and envelope equations are coupled and must be solved simultaneously
- Image terms contain nonlinear terms that can be difficult to evaluate explicitly
  - Aperture geometry changes image correction
- The formulation is not self-consistent because a charge profile is assumed
  - Uniform density choice motivated by KV results and Debye screening
  - The assumed distribution form not evolving represents a fluid model closure
- Constant (normalized when accelerating) emittances are generally assumed

$$Q = \frac{q\lambda}{2\pi m\epsilon_0\gamma_b^3\beta_b^2c^2} \qquad \varepsilon_{nx} = \gamma_b\beta_b\varepsilon_x = \mathrm{const}$$

$$\varepsilon_{nx} = \gamma_b\beta_b\varepsilon_x = \mathrm{const}$$

β_b, γ_b, λ specified by “acceleration schedule”

S3: Centroid Equations of Motion

Neglect image charge terms, then the centroid equation of motion becomes:

$$\boxed{X'' + \frac{(\gamma_b \beta_b)'}{(\gamma_b \beta_b)} X' + \kappa_x X = 0}$$

- Usual Hill's equation with additional acceleration term
- Single particle form and usual phase amplitude methods, Courant-Snyder invariants, and stability bounds can be immediately applied

$\boxed{\sigma_{0x} < 180^\circ}$ centroid stability, 1st stability condition

Example: FODO channel centroid evolution

Mid-drift launch:

$X(0) = 1$ mm
$X'(0) = 1$ mrad

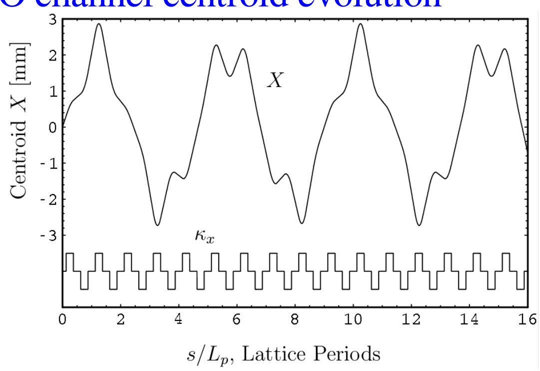

lattice/beam parameters:

$\beta_b = \text{const}$
$\sigma_0 = 80^\circ$
$L_p = 0.5$ m
$\eta = 0.5$

Driving Errors:

The reference orbit is ideally tuned for zero centroid offset. But there will always be driving errors that will cause the centroid oscillations to accumulate with beam propagation distance:

$$\boxed{X'' + \frac{(\gamma_b \beta_b)'}{(\gamma_b \beta_b)} X' + \frac{G_n}{G_0} \kappa_q(s) X = \frac{G_n}{G_0} \kappa_q(s) \Delta_{xn}}$$

$\frac{G_n}{G_0} =$ nth quadrupole gradient error (1 = no error)

$\Delta_{xn} =$ nth quadrupole transverse displacement error

Example: FODO channel centroid with quadrupole displacement errors

$\frac{G_n}{G_0} = 1$
$\Delta_{xn} = [-0.5, 0.5]$ mm
(uniform dist)

same lattice as previous

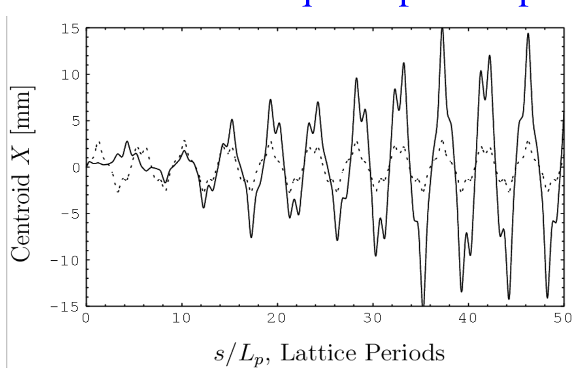

solid – with errors
dashed – no errors

Errors will result in a characteristic random walk increase in oscillation amplitude due to the driving terms.

Control by:

- Synthesize small applied dipole fields to regularly steer the centroid back on-axis
- Fabricate and align focusing elements with higher precision
- Employ a sufficiently large aperture to contain the oscillations and limit detrimental nonlinear image charge effects

Economics dictates the optimal strategy

Image Effects:

Model the beam as a displaced line-charge. Then the equations of motion are modified as:

$$\boxed{X'' + \frac{(\gamma_b \beta_b)'}{(\gamma_b \beta_b)} X' + \kappa_x X = \frac{QX}{r_p^2 - X^2}}$$

$$\frac{QX}{r_p^2 - X^2} \simeq \frac{Q}{r_p^2} X + \frac{Q}{r_p^4} X^3$$

linear correction Nonlinear correction (smaller)

Example: FODO channel centroid with image charge corrections

$r_p = 30$ mm

$Q = 2 \times 10^{-4}$

same lattice as previous

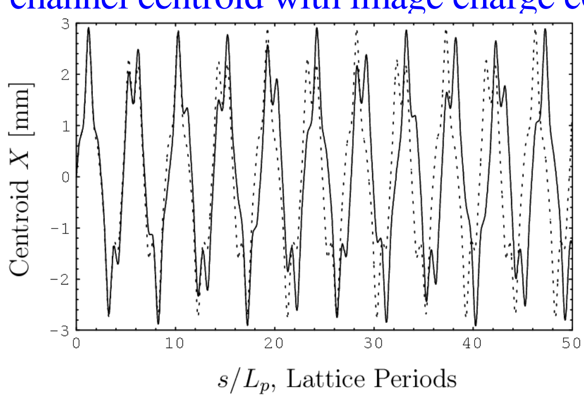

solid – with images

dashed – no images

Main effect appears to be an accumulated phase error of the centroid orbit since, generally the centroid error oscillations are not "matched" orbits. This will complicate extrapolations of errors over many lattice periods

Control by:

- Keeping centroid displacements small by correcting
- Make pipe larger
- Generally less problematic than alignment and excitation errors

General Comments:

- More detailed analyses show that the coupling of the envelope radii to the centroid evolution is often weak
- Fringe fields are more important for accurate calculation of centroid orbits since orbits are not part of a matched lattice
  - Nonideal orbits are poorly tuned to lattice and become more sensitive to the precise phase of impulses
- Over long path lengths many nonlinear terms can influence results
- Lattice errors are not often known so one must often analyze characteristic error distributions to see if centroids measured are consistent with expectations

S4: Envelope Equations of Motion

Overview

- Generally found that couplings to centroid displacements Δ_x Δ_y are weak
  - Centroid ideally zero
- Envelope eqns are most important in designing transverse focusing systems
  - Expresses average radial force balance
  - Unfortunately, can be difficult to analyze analytically for scaling
  - "Systems" codes generally written using envelope equations, stability criteria, and practical engineering constraints
- Instabilities of the envelope equations in periodic focusing lattices must be avoided in machine operation
  - Instabilities are strong and real
  - Represent lowest order "KV" modes of a full kinetic theory
- Previous derivation of envelope equations relied on Courant-Snyder invariants in linear applied and self-fields. Analysis shows that the same force balances result for a uniform elliptical beam with no image couplings.
  - Debye screening arguments suggest assumed uniform density model taken should be a good approximation for intense space-charge

KV/rms Envelope Equations

The envelope equation reflects low-order force balances:

$$r_x'' + \frac{(\gamma_b\beta_b)'}{(\gamma_b\beta_b)} r_x' + \kappa_x r_x - \frac{2Q}{r_x + r_y} - \frac{\varepsilon_x^2}{r_x^3} = 0$$

$$r_y'' + \frac{(\gamma_b\beta_b)'}{(\gamma_b\beta_b)} r_y' + \kappa_y r_y - \frac{2Q}{r_x + r_y} - \frac{\varepsilon_y^2}{r_y^3} = 0$$

Terms:	Applied Acceleration	Applied Focusing	Space-Charge Defocusing	Thermal Defocusing
	Lattice	Lattice	Perveance	Emittance

The "acceleration schedule" specifies both $\gamma_b\beta_b$ and λ then the equations are integrated with:

$$\boxed{\begin{aligned}\gamma_b\beta_b\varepsilon_x &= \text{const} \\ \gamma_b\beta_b\varepsilon_y &= \text{const}\end{aligned}}$$

normalized emittance conservation

$$\boxed{Q = \frac{q\lambda}{2\pi\epsilon_0 m\gamma_b^3\beta_b^2 c^2}}$$

specified perveance

Reminder: It was shown for a coasting beam that the envelope equations remain valid for elliptic charge densities suggesting more general validity [Sacherer, IEEE Trans. Nucl. Sci. 18, 1101 (1971), J.J. Barnard, Intro. Lectures]

For any beam with elliptic symmetry charge density in each transverse slice:

$$\boxed{\rho = \rho\left(\frac{x^2}{r_x^2} + \frac{y^2}{r_y^2}\right)}$$

Based on:

$$\langle x\frac{\partial\phi}{\partial x}\rangle_\perp = -\frac{\lambda}{4\pi\epsilon_0}\frac{r_x}{r_x + r_y}$$

see J.J. Barnard intro. lectures

the KV envelope equations

$$\boxed{\begin{aligned} r_x''(s) + \kappa_x(s) r_x(s) - \frac{2Q}{r_x(s) + r_y(s)} - \frac{\varepsilon_x^2(s)}{r_x^3(s)} &= 0 \\ r_y''(s) + \kappa_y(s) r_y(s) - \frac{2Q}{r_x(s) + r_y(s)} - \frac{\varepsilon_y^2(s)}{r_y^3(s)} &= 0 \end{aligned}}$$

remain valid when (averages taken with the full distribution):

$$Q = \frac{q\lambda}{2\pi\epsilon_0 m\gamma_b^3\beta_b^2 c^2} = \text{const} \qquad \lambda = q\int d^2x_\perp\, \rho \;=\; \text{const}$$

$$r_x = 2\langle x^2\rangle_\perp^{1/2} \qquad \varepsilon_x = 4[\langle x^2\rangle_\perp\langle x'^2\rangle_\perp - \langle xx'\rangle_\perp^2]^{1/2}$$

$$r_y = 2\langle y^2\rangle_\perp^{1/2} \qquad \varepsilon_y = 4[\langle y^2\rangle_\perp\langle y'^2\rangle_\perp - \langle yy'\rangle_\perp^2]^{1/2}$$

Properties of Envelope Equation Terms:

Applied Focusing and Acceleration: $\kappa_x r_x \qquad \frac{(\gamma_b\beta_b)'}{(\gamma_b\beta_b)} r'_x$

- Analogous to single particle orbit terms
- Contributions to beam envelope essentially the same as in single particle case
- Have strong s dependance, can be both focusing and defocusing
  - Act only in focusing elements and acceleration gaps

Perveance: $\frac{2Q}{r_x + r_y}$

- Acts continuously in s, always defocusing
- Becomes stronger (relatively to other terms) when the beam expands in cross-sectional area

Emittance: $\frac{\varepsilon_x^2}{r_x^3}$

- Acts continuously in s, always defocusing
- Becomes stronger (relatively to other terms) when the beam becomes small in cross-sectional area
- Scaling makes clear why it is necessary to inhibit emittance growth for applications where small spots are desired on target

As the beam expands, the perveance term will eventually dominate:

[see analytical analysis in: S.M. Lund and B. Bukh, PRSTAB 7, 024801 (2004)]

Free expansion $(\kappa_x = \kappa_y = 0)$

Initial conditions:

Space-Charge Dominated: $\varepsilon_x = 0$

Emittance Dominated: $Q = 0$

Initial Conditions

$$\frac{Q}{r_x(s_i)} = \frac{\varepsilon_x^2}{r_x^3(s_i)}$$

$$r'_x(s_i) = 0$$

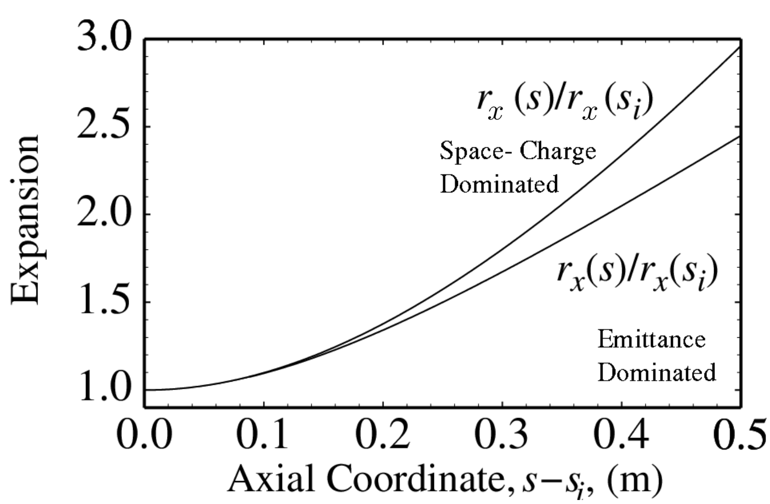

S5: Matched Envelope Solution:

Neglect acceleration $(\gamma_b \beta_b = \text{const})$ or use transformed variables:

$$\boxed{\begin{aligned} & r_x''(s) + \kappa_x(s) r_x(s) - \frac{2Q}{r_x(s) + r_y(s)} - \frac{\varepsilon_x^2}{r_x^3(s)} = 0 \\ & r_y''(s) + \kappa_y(s) r_y(s) - \frac{2Q}{r_x(s) + r_y(s)} - \frac{\varepsilon_y^2}{r_y^3(s)} = 0 \\ & r_x(s + L_p) = r_x(s) \qquad r_x(s) > 0 \\ & r_y(s + L_p) = r_y(s) \qquad r_y(s) > 0 \end{aligned}}$$

Matching involves finding specific initial conditions for the envelope to have the periodicity of the lattice:

Find Values of: $\boxed{\begin{matrix} r_x(s_i) & r_x'(s_i) \\ r_y(s_i) & r_y'(s_i) \end{matrix}}$ $\longrightarrow$ **Such That:** $\boxed{\begin{matrix} r_x(s_i + L_p) = r_x(s_i) & r_x'(s_i + L_p) = r_x'(s_i) \\ r_y(s_i + L_p) = r_y(s_i) & r_y'(s_i + L_p) = r_y'(s_i) \end{matrix}}$

- Typically constructed with numerical root finding from estimated/guessed values
  - Can be difficult in practice for complicated lattices, but well posed
- Recent iterative technique developed to numerically calculate without root finding
  [S.M. Lund, S. Chilton and E.P. Lee, PRSTAB **9**, 064201 (2006)]

Typical Matched vs Mismatched solution for FODO channel:

Matched

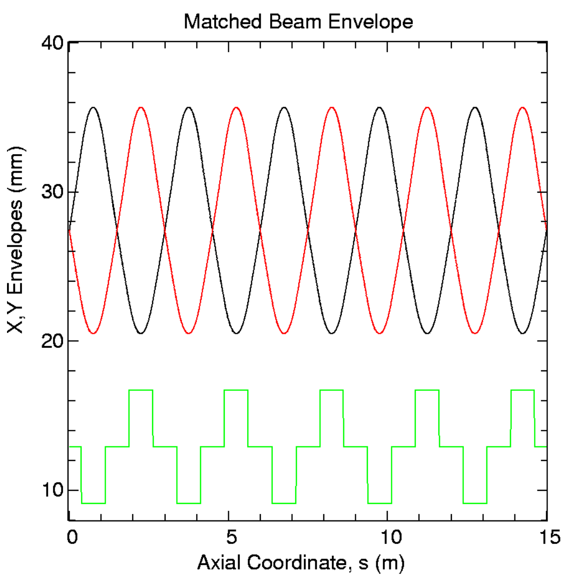

Mismatched

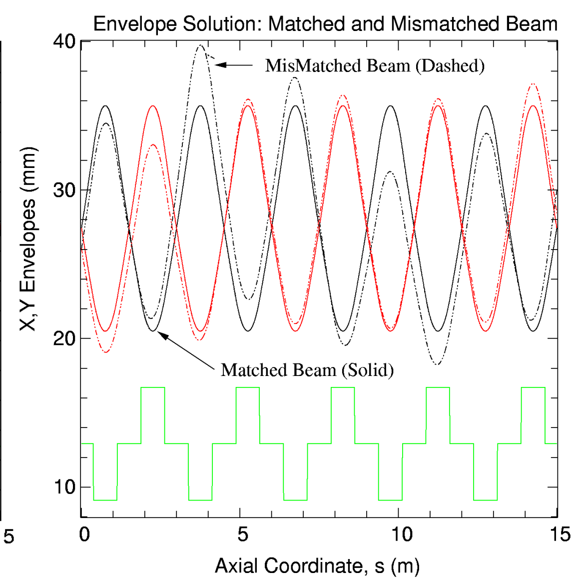

The matched beam is the most radially compact solution to the envelope equations rendering it highly important for beam transport

The matched solution to the KV envelope equations reflects the symmetry of the focusing lattice and must in general be calculated numerically

$$\boxed{\begin{aligned} r_x(s+L_p) &= r_x(s) \\ r_y(s+L_p) &= r_y(s) \\ \varepsilon_x &= \varepsilon_y \end{aligned}}$$

Parameters

$L_p = 0.5$ m, $\sigma_0 = 80°$, $\eta = 0.5$

$\varepsilon_x = 50$ mm-mrad

$\sigma/\sigma_0 = 0.2$

Solenoidal Focusing

$(Q = 6.6986 \times 10^{-4})$

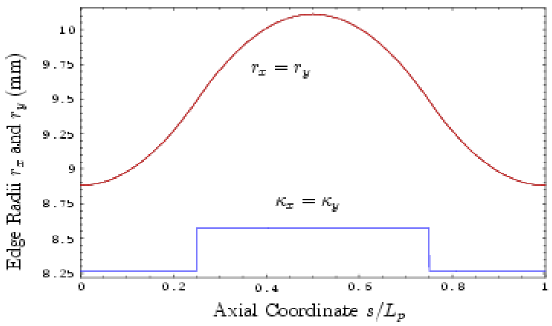

FODO Quadrupole Focusing

$(Q = 6.5614 \times 10^{-4})$

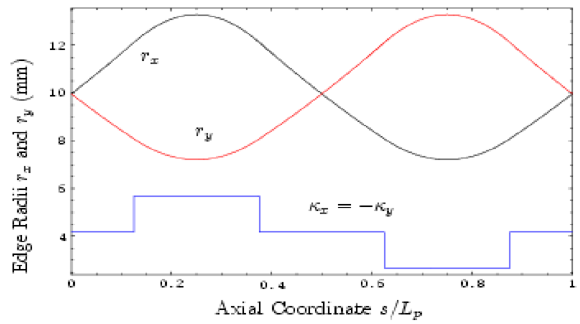

Symmetries of a matched beam are interpreted in terms of a local rms equivalent KV beam and moments/projections of the KV distribution

Projection

x-y

area: $\pi r_x r_y \neq$ const

x-x'

area: $\pi\varepsilon_x =$ const (CS Invariant)

y-y'

area: $\pi\varepsilon_y =$ const (CS Invariant)

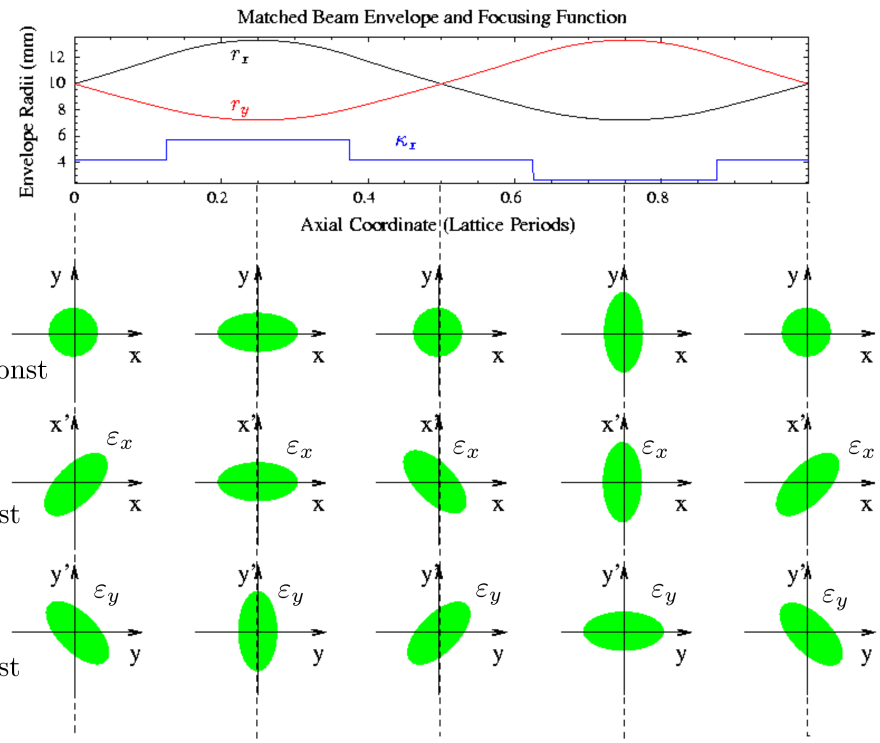

S6: Envelope Perturbations:

In the envelope equations set:

Envelope Perturbations:

$$r_x(s) = r_{xm}(s) + \delta r_x(s)$$
$$r_y(s) = r_{ym}(s) + \delta r_y(s)$$

Matched Envelope — Mismatch Perturbations

$$r_{xm}(s + L_p) = r_{xm}(s) \qquad r_{xm}(s) > 0$$
$$r_{ym}(s + L_p) = r_{ym}(s) \qquad r_{ym}(s) > 0$$

$$r_{xm}(s) \gg |\delta r_{xm}(s)|$$
$$r_{ym}(s) \gg |\delta r_{ym}(s)|$$

Driving Perturbations:

$$\kappa_x(s) \to \kappa_x(s) + \delta\kappa_x(s)$$
$$\kappa_y(s) \to \kappa_y(s) + \delta\kappa_y(s)$$
$$Q \to Q + \delta Q(s)$$
$$\varepsilon_x \to \varepsilon_x + \delta\varepsilon_x(s)$$
$$\varepsilon_y \to \varepsilon_y + \delta\varepsilon_y(s)$$

Amplitudes defined in terms of producing small envelope perturbations with:

$$r_{xm}(s) \gg |\delta r_{xm}(s)|$$
$$r_{ym}(s) \gg |\delta r_{ym}(s)|$$

- Driving terms and distribution errors drive envelope perturbations
  - Arise from many sources: focusing errors, lost particles, emittance growth, ...

The matched solution satisfies:

$$\boxed{\begin{aligned} & r''_{xm}(s) + \kappa_x(s) r_{xm}(s) - \frac{2Q}{r_{xm}(s) + r_{ym}(s)} - \frac{\varepsilon_x^2}{r_{xm}^3(s)} = 0 \\ & r''_{ym}(s) + \kappa_y(s) r_{ym}(s) - \frac{2Q}{r_{xm}(s) + r_{ym}(s)} - \frac{\varepsilon_y^2}{r_{ym}^3(s)} = 0 \\ & r_{xm}(s + L_p) = r_{xm}(s) \qquad r_{xm}(s) > 0 \\ & r_{ym}(s + L_p) = r_{ym}(s) \qquad r_{ym}(s) > 0 \end{aligned}}$$

Linearized Perturbed Envelope Equations:

$$\boxed{\begin{aligned}\delta r_x'' + \kappa_x \delta r_x + \frac{2Q}{(r_{xm}+r_{ym})^2}(\delta r_x + \delta r_y) + \frac{3\varepsilon_x^2}{r_{xm}^4}\delta r_x \\ = -r_{xm}\delta\kappa_x + \frac{2}{r_{xm}+r_{ym}}\delta Q + \frac{2\varepsilon_x^2}{r_{xm}^3}\delta\varepsilon_x \\ \delta r_y'' + \kappa_y \delta r_y + \frac{2Q}{(r_{xm}+r_{ym})^2}(\delta r_x + \delta r_y) + \frac{3\varepsilon_y^2}{r_{ym}^4}\delta r_y \\ = -r_{ym}\delta\kappa_y + \frac{2}{r_{xm}+r_{ym}}\delta Q + \frac{2\varepsilon_y^2}{r_{ym}^3}\delta\varepsilon_y\end{aligned}}$$

Homogeneous Equations:

$$\boxed{\begin{aligned}\delta r_x'' + \kappa_x \delta r_x + \frac{2Q}{(r_{xm}+r_{ym})^2}(\delta r_x + \delta r_y) + \frac{3\varepsilon_x^2}{r_{xm}^4}\delta r_x = 0 \\ \delta r_y'' + \kappa_y \delta r_y + \frac{2Q}{(r_{xm}+r_{ym})^2}(\delta r_x + \delta r_y) + \frac{3\varepsilon_y^2}{r_{ym}^4}\delta r_y = 0\end{aligned}}$$

Vector Form of the Linearized Perturbed Envelope Equations:

$$\boxed{\frac{d}{ds}\delta\mathbf{R} + \mathbf{K}\cdot\delta\mathbf{R} = \delta\mathbf{P}}$$

$$\delta\mathbf{R} \equiv \begin{pmatrix}\delta r_x \\ \delta r_x' \\ \delta r_y \\ \delta r_y'\end{pmatrix}$$ Coordinate vector

Coefficient matrix

$$\mathbf{K} \equiv \begin{pmatrix} 0 & -1 & 0 & 0 \\ k_{xm} & 0 & k_{0m} & 0 \\ 0 & 0 & 0 & -1 \\ k_{0m} & 0 & k_{ym} & 0 \end{pmatrix}$$

$$k_{0m} = \frac{2Q}{(r_{xm}+r_{ym})^2}$$

$$k_{jm} = \kappa_j + 3\frac{\varepsilon_j^2}{r_{jm}^4} + k_{0m} \qquad j = x,\ y$$

$$\delta\mathbf{P} \equiv \begin{pmatrix} 0 \\ -\delta\kappa_x + 2\frac{\delta Q}{r_{xm}+r_{ym}} + 2\frac{\varepsilon_x\delta\varepsilon_x}{r_{xm}^3} \\ 0 \\ -\delta\kappa_y + 2\frac{\delta Q}{r_{xm}+r_{ym}} + 2\frac{\varepsilon_y\delta\varepsilon_y}{r_{ym}^3}\end{pmatrix}$$ Driving perturbation vector

Expand solution into homogeneous and particular parts:

$$\delta\mathbf{R} = \delta\mathbf{R}_h + \delta\mathbf{R}_p$$

$\delta\mathbf{R}_h =$ homogeneous solution

$\delta\mathbf{R}_p =$ particular solution

$$\frac{d}{ds}\delta\mathbf{R}_h + \mathbf{K}\cdot\delta\mathbf{R}_h = 0 \qquad \frac{d}{ds}\delta\mathbf{R}_p + \mathbf{K}\cdot\delta\mathbf{R}_p = \delta\mathbf{P}$$

Homogeneous Solution:

- Describes normal mode oscillations
- Original analysis by Struckmeier and Reiser [Part. Accel. **14**, 227 (1984)]

Particular Solution:

- Describes action of driving terms
- Characterize in terms of projections on homogeneous response

Homogeneous solution expressible as a map:

$$\boxed{\begin{aligned}\delta\vec{R}(s) &= \mathbf{M}_e(s|s_i)\cdot\delta\vec{R}(s_i)\\ \delta\vec{R}(s) &= (\delta r_x, \delta r_x', \delta r_y, \delta r_y')\\ \mathbf{M}_e(s|s_i) &= 4\times 4 \text{ transfer map.}\end{aligned}}$$

Analogous to the 2x2 analysis of Hill's equation

Eigenvalues and eigenvectors of map through one period describe normal modes and stability properties:

$$\boxed{\mathbf{M}_e(s_i + L_p|s_i)\cdot\vec{E}_n(s_i) = \lambda_n\vec{E}_n(s_i)}$$

Stability

$$\boxed{\lambda_n = \gamma_n e^{i\sigma_n} \quad \begin{array}{ll}\sigma_n \to & \text{mode phase advance (real)}\\ \gamma_n \to & \text{mode growth factor (real)}\end{array}}$$

Mode Expansion/Launching

$$\boxed{\begin{gathered}\delta\vec{R}(s_i) = \sum_{n=1}^{4}\alpha_n\vec{E}_n(s_i)\\ \alpha_n = \text{const}\end{gathered}}$$

Eigenvalue/Eigenvector Symmetry Classes:

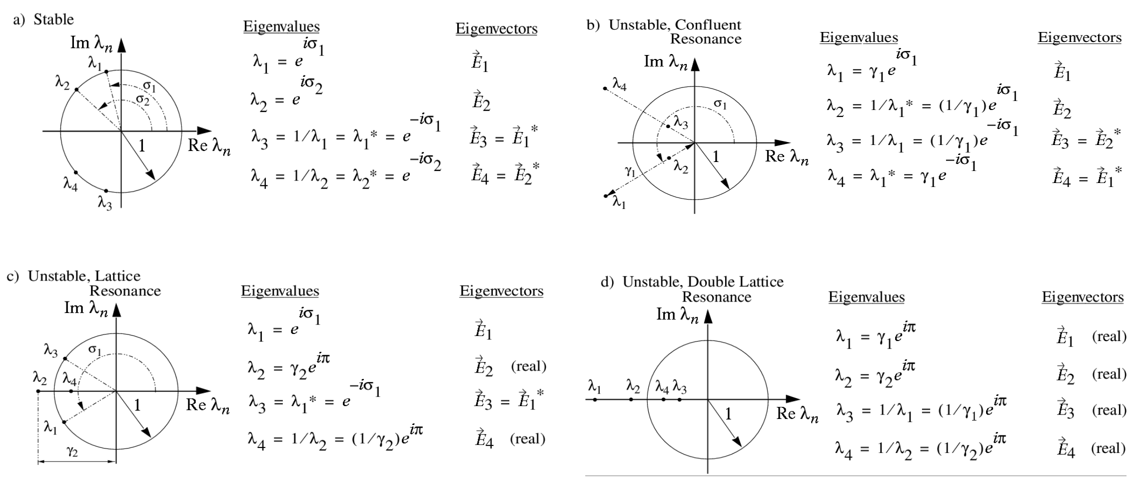

Symmetry classes of eigenvalues/eigenvectors:

- Determine normal mode symmetries
- See A. Dragt, Lectures on Nonlinear Orbit Dynamics, in Physics of High Energy Particle Accelerators, (AIP Conf. Proc. No. 87, 1982, p. 147)

Pure mode launching conditions:

Launching conditions for distinct normal modes corresponding to the eigenvalue classes illustrated:

$$A_\ell = \text{ mode amplitude (real)} \qquad \ell = \text{ mode index}$$
$$\psi_\ell = \text{ mode launch phase (real)}$$

Case	Mode	Launching Condition	Lattice Period Advance
(a) Stable	1 - Stable Osc.	$\delta\mathbf{R}_1 = A_1 e^{i\psi_1}\mathbf{E}_1 + \text{C.C.}$	$\mathbf{M}_e\delta\mathbf{R}_1(\psi_1) = \delta\mathbf{R}_1(\psi_1+\sigma_1)$
	2 - Stable Osc.	$\delta\mathbf{R}_2 = A_2 e^{i\psi_2}\mathbf{E}_2 + \text{C.C.}$	$\mathbf{M}_e\delta\mathbf{R}_2(\psi_2) = \delta\mathbf{R}_2(\psi_2+\sigma_2)$
(b) Unstable Confluent Res.	1 - Exp. Growth	$\delta\mathbf{R}_1 = A_1 e^{i\psi_1}\mathbf{E}_1 + \text{C.C.}$	$\mathbf{M}_e\delta\mathbf{R}_1(\psi_1) = \gamma_1\delta\mathbf{R}_1(\psi_1+\sigma_1)$
	2 - Exp. Damping	$\delta\mathbf{R}_2 = A_2 e^{i\psi_2}\mathbf{E}_2 + \text{C.C.}$	$\mathbf{M}_e\delta\mathbf{R}_2(\psi_2) = (1/\gamma_1)\delta\mathbf{R}_2(\psi_2+\sigma_1)$
(c) Unstable Lattice Res.	1 - Stable Osc.	$\delta\mathbf{R}_1 = A_1 e^{i\psi_1}\mathbf{E}_1 + \text{C.C.}$	$\mathbf{M}_e\delta\mathbf{R}_1(\psi_1) = \delta\mathbf{R}_1(\psi_1+\sigma_1)$
	2 - Exp. Growth	$\delta\mathbf{R}_2 = A_2\mathbf{E}_2$	$\mathbf{M}_e\delta\mathbf{R}_2 = -\gamma_2\delta\mathbf{R}_2$
	3 - Exp. Damping	$\delta\mathbf{R}_3 = A_3\mathbf{E}_4$	$\mathbf{M}_e\delta\mathbf{R}_3 = -(1/\gamma_2)\delta\mathbf{R}_3$
(d) Unstable Double Lattice Resonance	1 - Exp. Growth	$\delta\mathbf{R}_1 = A_1\mathbf{E}_1$	$\mathbf{M}_e\delta\mathbf{R}_1 = -\gamma_1\delta\mathbf{R}_1$
	2 - Exp. Growth	$\delta\mathbf{R}_2 = A_2\mathbf{E}_2$	$\mathbf{M}_e\delta\mathbf{R}_2 = -\gamma_2\delta\mathbf{R}_2$
	3 - Exp. Damping	$\delta\mathbf{R}_3 = A_3\mathbf{E}_3$	$\mathbf{M}_e\delta\mathbf{R}_3 = -(1/\gamma_1)\delta\mathbf{R}_3$
	4 - Exp. Damping	$\delta\mathbf{R}_4 = A_4\mathbf{E}_4$	$\mathbf{M}_e\delta\mathbf{R}_4 = -(1/\gamma_2)\delta\mathbf{R}_4$

$$\delta\vec{R}_\ell \equiv \delta\vec{R}_\ell(s_i), \quad \vec{E}_\ell \equiv \vec{E}_\ell(s_i), \quad \text{and} \quad \mathbf{M}_e \equiv \mathbf{M}_e(s_i+L_p|s_i)$$

$$\delta\mathbf{R}(s) = \begin{cases} A_1[\mathbf{E}_1(s)e^{i\psi_1(s)} + \mathbf{E}_1^*(s)e^{-i\psi_1(s)}] + A_2[\mathbf{E}_2(s)e^{i\psi_2(s)} + \mathbf{E}_2^*(s)e^{-i\psi_2(s)}], & \text{cases (a) and (b)}, \\ A_1[\mathbf{E}_1(s)e^{i\psi_1(s)} + \mathbf{E}_1^*(s)e^{-i\psi_1(s)}] + A_2\mathbf{E}_2(s) + A_3\mathbf{E}_4(s), & \text{case (c)}, \\ A_1\mathbf{E}_1(s) + A_2\mathbf{E}_2(s) + A_3\mathbf{E}_3(s) + A_4\mathbf{E}_4(s), & \text{case (d)}, \end{cases}$$

Decoupled Modes

In a continuous or periodic solenoidal focusing channel

$$\kappa_x(s) = \kappa_y(s) = \kappa(s)$$

with a round matched-beam solution

$$\varepsilon_x = \varepsilon_y = \varepsilon = \text{const}$$
$$r_{xm}(s) = r_{ym}(s) = r_m(s)$$

envelope perturbations are simply decoupled with:

$$\delta r_+(s) = \frac{\delta r_x(s) + \delta r_y(s)}{2} \qquad \text{Breathing Mode}$$
$$\delta r_-(s) = \frac{\delta r_x(s) - \delta r_y(s)}{2} \qquad \text{Quadrupole Mode}$$

$$\delta r_+'' + \kappa\,\delta r_+ + \frac{2Q}{r_m^2}\delta r_+ + \frac{3\varepsilon^2}{r_m^4}\delta r_+ = -r_m\left(\frac{\delta\kappa_x + \delta\kappa_y}{2}\right) + \frac{1}{r_m}\delta Q + \frac{2\varepsilon^2}{r_m^3}\left(\frac{\delta\varepsilon_x + \delta\varepsilon_y}{2}\right)$$
$$\delta r_-'' + \kappa\,\delta r_- + \frac{3\varepsilon^2}{r_m^4}\delta r_- = -r_m\left(\frac{\delta\kappa_x - \delta\kappa_y}{2}\right) + \frac{2\varepsilon^2}{r_m^3}\left(\frac{\delta\varepsilon_x - \delta\varepsilon_y}{2}\right)$$

Decoupled Mode Properties:

Space charge terms ~ Q only directly expressed in equation for $\delta r_+(s)$

- Indirectly present in both equations from matched envelope $r_m(s)$

Homogeneous Solution:

- Restoring term for $\delta r_+(s)$ larger than for $\delta r_-(s)$
  - Breathing mode oscillates faster than quadrupole mode

Particular Solution:

- Misbalances in focusing and emittance driving terms can project onto either mode
  - nonzero perturbed $\kappa_x(s) + \kappa_y(s)$ and $\varepsilon_x(s) + \varepsilon_y(s)$ project onto breathing mode
  - nonzero perturbed $\kappa_x(s) - \kappa_y(s)$ and $\varepsilon_x(s) - \varepsilon_y(s)$ project onto quadrupole mode
- Perveance driving perturbations project only on breathing mode

Previous symmetry classes greatly reduce for decoupled modes:

Previous homogeneous 4x4 solution map:

$$\delta\vec{R}(s) = \mathbf{M}_e(s|s_i)\cdot\delta\vec{R}(s_i)$$
$$\delta\vec{R}(s) = (\delta r_x, \delta r_x', \delta r_y, \delta r_y')$$
$$\mathbf{M}_e(s|s_i) = 4\times 4 \text{ transfer map.}$$

greatly reduces to two independent 2x2 maps:

$$\boxed{\begin{aligned}&\delta\mathbf{R} \equiv (\delta r_+, \delta r_+', \delta r_-, \delta r_-')\\ &\mathbf{M}_e(s_i+L_p|s_i) = \begin{bmatrix}\mathbf{M}_+(s_i+L_p|s_i) & 0\\ 0 & \mathbf{M}_-(s_i+L_p|s_i)\end{bmatrix}\end{aligned}}$$

with corresponding eigenvalue problems:

$$\boxed{\mathbf{M}_\pm(s_i+L_p|s_i)\cdot\mathbf{E}_n(s_i) = \lambda_\pm\mathbf{E}_n(s_i)}$$

Many familiar results from analysis of Hills equation can be immediately applied to the decoupled case, for example:

$$\frac{1}{2}|\text{Tr }\mathbf{M}_\pm(s_i+L_p|s_i)| < 1 \longrightarrow \text{mode stability}$$

Eigenvalue symmetries and launching conditions simplify for decoupled modes

Eigenvalue Symmetry 1:

Stable

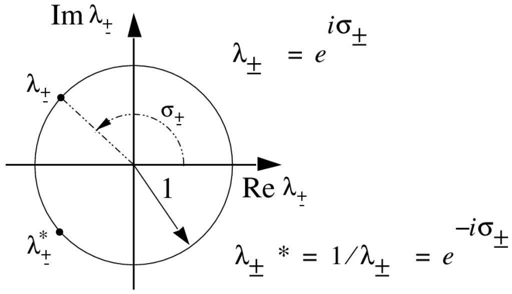

Eigenvalue Symmetry 2:

Unstable, Lattice Resonance

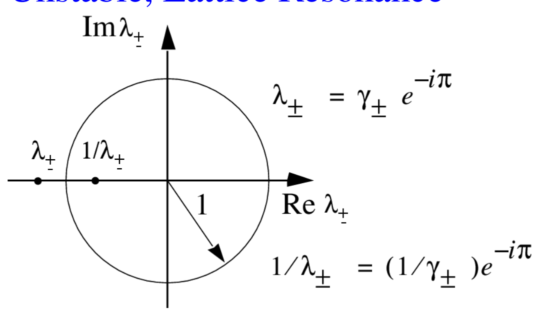

Launching Condition / Projections

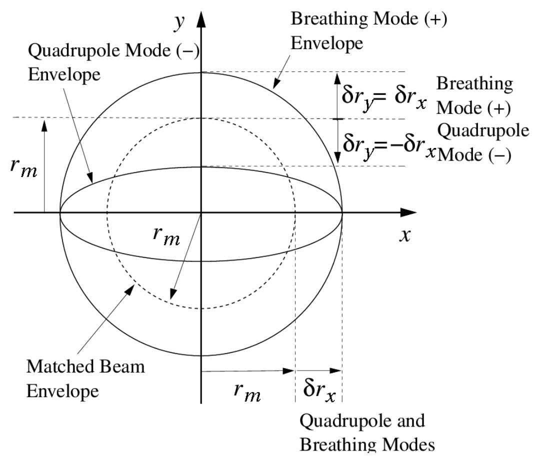

General Mode Limits

Using phase-amplitude analysis can show for any linear focusing lattice:

1) Phase advance of any normal mode satisfies the zero space-charge limit:

$$\boxed{\lim_{Q\to 0} \sigma_\ell = 2\sigma_0}$$

2) Pure normal modes evolve with a quadratic phase-space (Courant-Snyder) invariant in the normal coordinates of the mode

Simply expressed for decoupled modes:

$$\boxed{\left[\frac{\delta r_\pm(s)}{w_\pm(s)}\right]^2 + \left[w'_\pm(s)\delta r_\pm(s) - w_\pm(s)\delta r'_\pm(s)\right]^2 = \text{const}}$$

where

$$w''_+(s) + \kappa(s)\, w_+(s) + \frac{2Q}{r_m^2(s)} w_+(s) + \frac{3\varepsilon^2}{r_m^4(s)} w_+(s) - \frac{1}{w_+^3(s)} = 0$$

$$w''_-(s) + \kappa(s)\, w_-(s) + \frac{3\varepsilon^2}{r_m^4(s)} w_-(s) - \frac{1}{w_-^3(s)} = 0$$

$$w_\pm(s + L_p) = w_\pm(s)$$

Analogous for coupled modes [See Edwards and Teng applies, IEEE Trans Nuc. Sci. **20**, 885 (1973)]

S7: Envelope Modes in Continuous Focusing

Focusing:

$$\kappa_x(s) = \kappa_y(s) = k_{\beta 0}^2 = \left(\frac{\sigma_0}{L_p}\right)^2 = \text{const}$$

Matched beam:

symmetric beam:

$$\varepsilon_x = \varepsilon_y = \varepsilon = \text{const}$$
$$r_{xm}(s) = r_{ym}(s) = r_m(s)$$

match condition:

$$k_{\beta 0}^2 r_m - \frac{Q}{r_m} - \frac{\varepsilon^2}{r_m^3} = 0$$

depressed phase advance:

$$\sigma = \sqrt{\sigma_0^2 - \frac{Q}{(r_m/L_p)^2}} = \frac{\varepsilon L_p}{r_m^2}$$

one parameter needed for scaled solution:

$$\frac{k_{\beta 0}^2 \varepsilon^2}{Q^2} = \frac{\sigma_0^2 \varepsilon^2}{Q^2 L_p^2} = \frac{(\sigma/\sigma_0)^2}{[1-(\sigma/\sigma_0)^2]^2}.$$

Decoupled Modes:

$$\delta r_\pm(s) = \frac{\delta r_x(s) \pm \delta r_y(s)}{2}$$

Envelope equations of motion become:

$$\boxed{\begin{aligned} L_p^2 \frac{d^2}{ds^2}\left(\frac{\delta r_+}{r_m}\right) + \sigma_+^2 \left(\frac{\delta r_+}{r_m}\right) &= -\frac{\sigma_0^2}{2}\left(\frac{\delta\kappa_x}{k_{\beta 0}^2} + \frac{\delta\kappa_y}{k_{\beta 0}^2}\right) + (\sigma_0^2 - \sigma^2)\frac{\delta Q}{Q} + \sigma^2\left(\frac{\delta\varepsilon_x}{\varepsilon} + \frac{\delta\varepsilon_y}{\varepsilon}\right) \\ L_p^2 \frac{d^2}{ds^2}\left(\frac{\delta r_-}{r_m}\right) + \sigma_-^2 \left(\frac{\delta r_-}{r_m}\right) &= -\frac{\sigma_0^2}{2}\left(\frac{\delta\kappa_x}{k_{\beta 0}^2} - \frac{\delta\kappa_y}{k_{\beta 0}^2}\right) + \sigma^2\left(\frac{\delta\varepsilon_x}{\varepsilon} - \frac{\delta\varepsilon_y}{\varepsilon}\right) \end{aligned}}$$

$\sigma_+ \equiv \sqrt{2\sigma_0^2 + 2\sigma^2}$ "breathing" mode phase advance

$\sigma_- \equiv \sqrt{\sigma_0^2 + 3\sigma^2}$ "quadrupole" mode phase advance

Homogeneous Solution (normal modes):

$$\boxed{\delta r_\pm(s) = \delta r_\pm(s_i)\cos\left(\sigma_\pm \frac{s-s_i}{L_p}\right) + \frac{\delta r'_\pm(s_i)}{\sigma_\pm/L_p}\sin\left(\sigma_\pm \frac{s-s_i}{L_p}\right)}$$

Mode Phase Advances

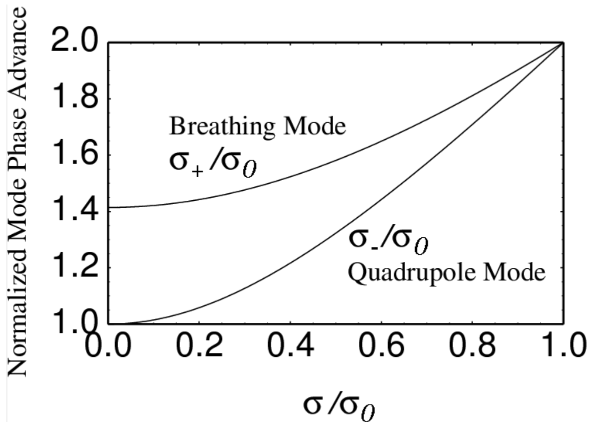

Mode Projections

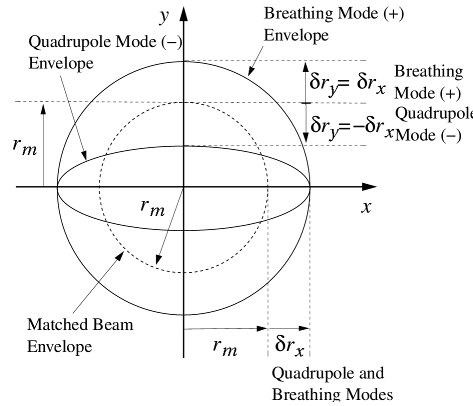

Particular Solution (driving perturbations):

Green's function form of solution:

$$\frac{\delta r_\pm(s)}{r_m} = \frac{1}{L_p^2}\int_{s_i}^{s} d\tilde{s}\; G_\pm(s,\tilde{s})\delta p_\pm(\tilde{s})$$

$$\delta p_+(s) = -\frac{\sigma_0^2}{2}\left[\frac{\delta\kappa_x(s)}{k_{\beta 0}^2} + \frac{\delta\kappa_y(s)}{k_{\beta 0}^2}\right] + (\sigma_0^2 - \sigma^2)\frac{\delta Q(s)}{Q} + \sigma^2\left[\frac{\delta\varepsilon_x(s)}{\varepsilon} + \frac{\delta\varepsilon_y(s)}{\varepsilon}\right]$$

$$\delta p_-(s) = -\frac{\sigma_0^2}{2}\left[\frac{\delta\kappa_x(s)}{k_{\beta 0}^2} - \frac{\delta\kappa_y(s)}{k_{\beta 0}^2}\right] + \sigma^2\left[\frac{\delta\varepsilon_x(s)}{\varepsilon} - \frac{\delta\varepsilon_y(s)}{\varepsilon}\right]$$

$$G_\pm(s,\tilde{s}) = \frac{1}{\sigma_\pm/L_p}\sin\left(\sigma_\pm\frac{s-\tilde{s}}{L_p}\right)$$

Green's function solution is fully general. Insight gained from simplified solutions for specific classes of driving perturbations:

- Adiabatic
- Sudden

covered here

- Ramped
- Harmonic

covered in PRSTAB review article

Continuous Focusing – adiabatic particular solution

For driving perturbations $\delta p_+(s)$ and $\delta p_-(s)$ slow on quadrupole mode wavelength ~ $2\pi L_p/\sigma_-$ the solution is:

Focusing

Perveance

$$
\begin{aligned}
\frac{\delta r_+(s)}{r_m} &= \frac{\delta p_+(s)}{\sigma_+^2} \\
&= -\left[\frac{1}{2}\frac{1}{1+(\sigma/\sigma_0)^2}\right]\frac{1}{2}\left(\frac{\delta\kappa_x(s)}{k_{\beta0}^2}+\frac{\delta\kappa_y(s)}{k_{\beta0}^2}\right)+\left[\frac{1}{2}\frac{1-(\sigma/\sigma_0)^2}{1+(\sigma/\sigma_0)^2}\right]\frac{\delta Q(s)}{Q} \\
&\quad+\left[\frac{(\sigma/\sigma_0)^2}{1+(\sigma/\sigma_0)^2}\right]\frac{1}{2}\left(\frac{\delta\varepsilon_x(s)}{\varepsilon}+\frac{\delta\varepsilon_y(s)}{\varepsilon}\right)
\end{aligned}
$$

Emittance

Coefficients of adiabatic terms in square brackets"[ ]"

Focusing

$$
\begin{aligned}
\frac{\delta r_-(s)}{r_m} &= \frac{\delta p_-(s)}{\sigma_-^2} \\
&= -\left[\frac{1}{1+3(\sigma/\sigma_0)^2}\right]\frac{1}{2}\left(\frac{\delta\kappa_x(s)}{k_{\beta0}^2}-\frac{\delta\kappa_y(s)}{k_{\beta0}^2}\right) \\
&\quad+\left[\frac{2(\sigma/\sigma_0)^2}{1+3(\sigma/\sigma_0)^2}\right]\frac{1}{2}\left(\frac{\delta\varepsilon_x(s)}{\varepsilon}-\frac{\delta\varepsilon_y(s)}{\varepsilon}\right)
\end{aligned}
$$

Emittance

Continuous Focusing – adiabatic solution coefficients

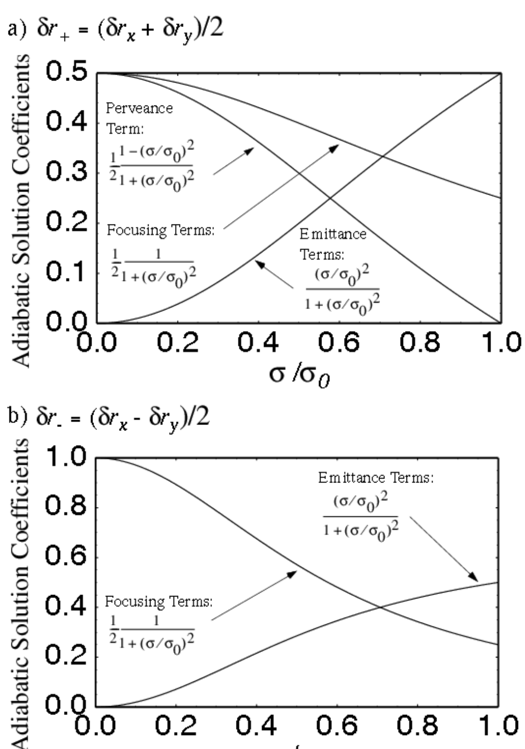

Relative strength of:

- Space-Charge (Perveance)
- Applied Focusing
- Emittance

terms vary with space-charge depression (σ/σ_0) for both breathing and quadrupole modes.

Continuous Focusing – sudden particular solution

For step function driving perturbations of form:

$$\boxed{\delta p_{\pm}(s) = \widehat{\delta p_{\pm}}\Theta(s - s_p)}$$

$s = s_p =$ axial coordinate perturbation applied

with amplitudes:

$$\widehat{\delta p_{+}} = -\frac{\sigma_0^2}{2}\left[\frac{\widehat{\delta\kappa_x}}{k_{\beta 0}^2} + \frac{\widehat{\delta\kappa_y}}{k_{\beta 0}^2}\right] + (\sigma_0^2 - \sigma^2)\frac{\widehat{\delta Q}}{Q} + \sigma^2\left[\frac{\widehat{\delta\varepsilon_x}}{\varepsilon} + \frac{\widehat{\delta\varepsilon_y}}{\varepsilon}\right] = \text{const}$$

$$\widehat{\delta p_{-}} = -\frac{\sigma_0^2}{2}\left[\frac{\widehat{\delta\kappa_x}}{k_{\beta 0}^2} - \frac{\widehat{\delta\kappa_y}}{k_{\beta 0}^2}\right] + \sigma^2\left[\frac{\widehat{\delta\varepsilon_x}}{\varepsilon} - \frac{\widehat{\delta\varepsilon_y}}{\varepsilon}\right] = \text{const}$$

The solution is given by the substitution in the expression for the adiabatic solution:

$$\boxed{\delta p_{\pm}(s) \rightarrow \widehat{\delta p_{\pm}}\left[1 - \cos\left(\sigma_{\pm}\frac{s - s_p}{L_p}\right)\right]\Theta(s - s_p)}$$

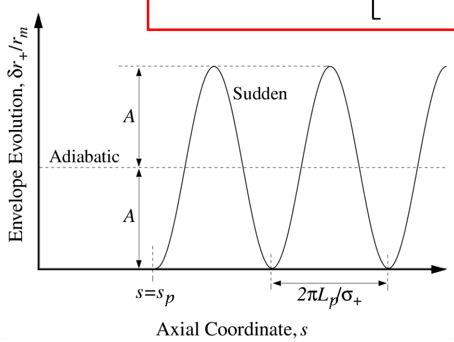

2x Excursion

Adiabatic Excursion

For the same amplitude of total driving perturbations, sudden perturbations result in 2x the envelope excursion that adiabatic perturbations produce.

S8: Envelope Modes in Periodic Focusing Channels

Overview

- Much more complicated the continuous limit results
  - Lattice can couple to oscillations and destabilize the system
  - Broad parametric instability can result
- Instability bands calculated will exclude wide ranges of parameter space from machine operation
  - Exclusion region depends on focusing type

Solenoidal Focusing – Matched Envelope Solution

a) σ_0 = 80° and η = 0.75

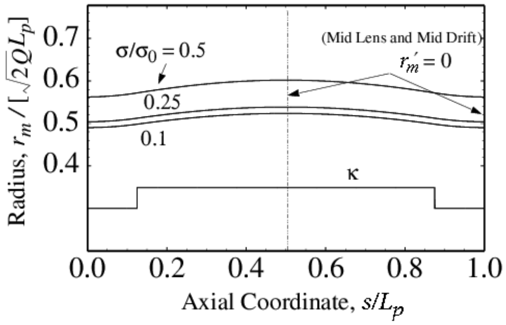

b) σ_0 = 80° and η = 0.25

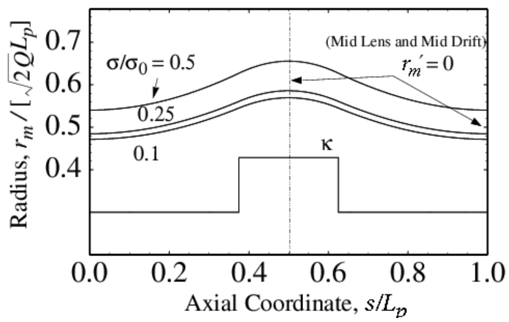

Focusing:

$$\kappa_x(s) = \kappa_y(s) = \kappa(s)$$

$$\kappa(s + L_p) = \kappa(s)$$

Matched Beam:

$$\varepsilon_x = \varepsilon_y = \varepsilon = \text{const}$$
$$r_{xm}(s) = r_{ym}(s) = r_m(s)$$

$$r_m(s + L_p) = r_m(s)$$

Using a transfer matrix approach on undepressed single-particle orbits set the strength of the focusing function for specified undepressed particle phase advance:

Solenoidal Focusing:

$$\cos\sigma_0 = \cos(2\Theta) - \frac{1-\eta}{\eta}\Theta\sin(2\Theta)$$

$$\Theta \equiv \frac{\sqrt{\hat{\kappa}}L_p}{2}$$

Solenoidal Focusing – parametric plots of breathing and quadrupole envelope mode phase advances two values of undepressed phase advance

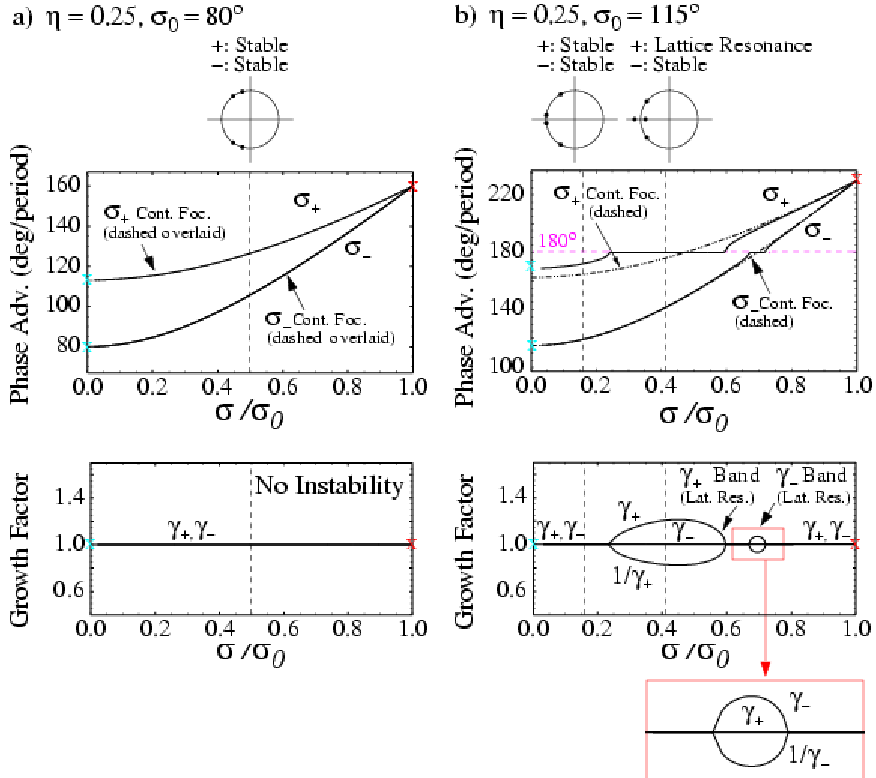

Solenoidal Focusing – mode instability bands become wider and stronger for smaller occupancy

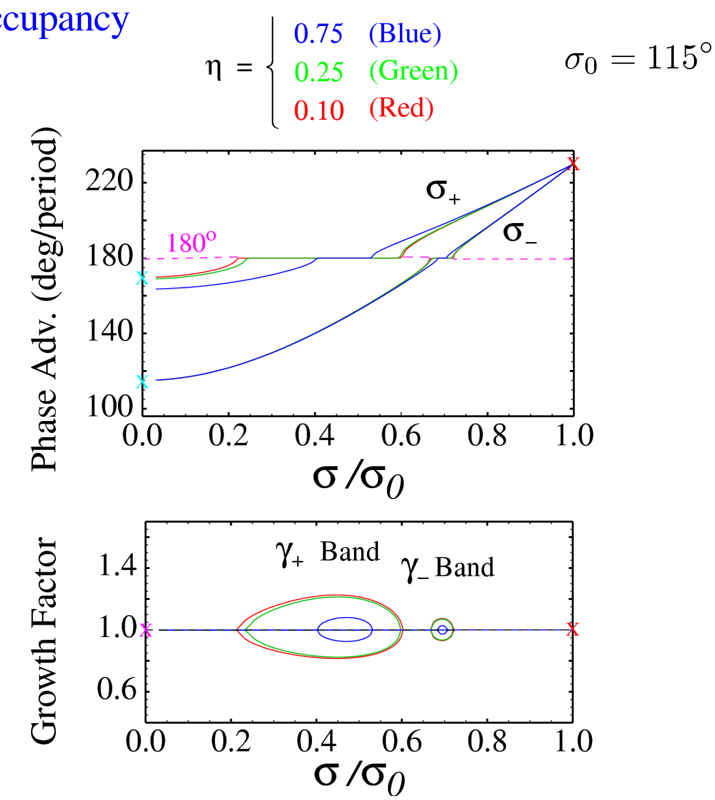

Solenoidal Focusing – broad ranges of parametric instability are found for the breathing and quadrupole bands that must be avoided in machine operation

$\eta = 0.75$ $\eta = 0.25$

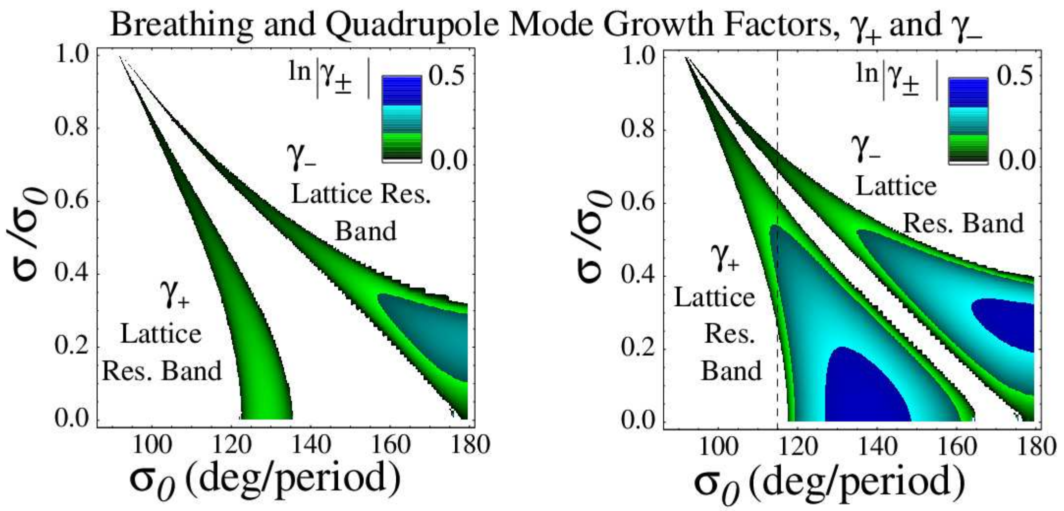

Solenoidal Focusing – parametric mode properties of band oscillations

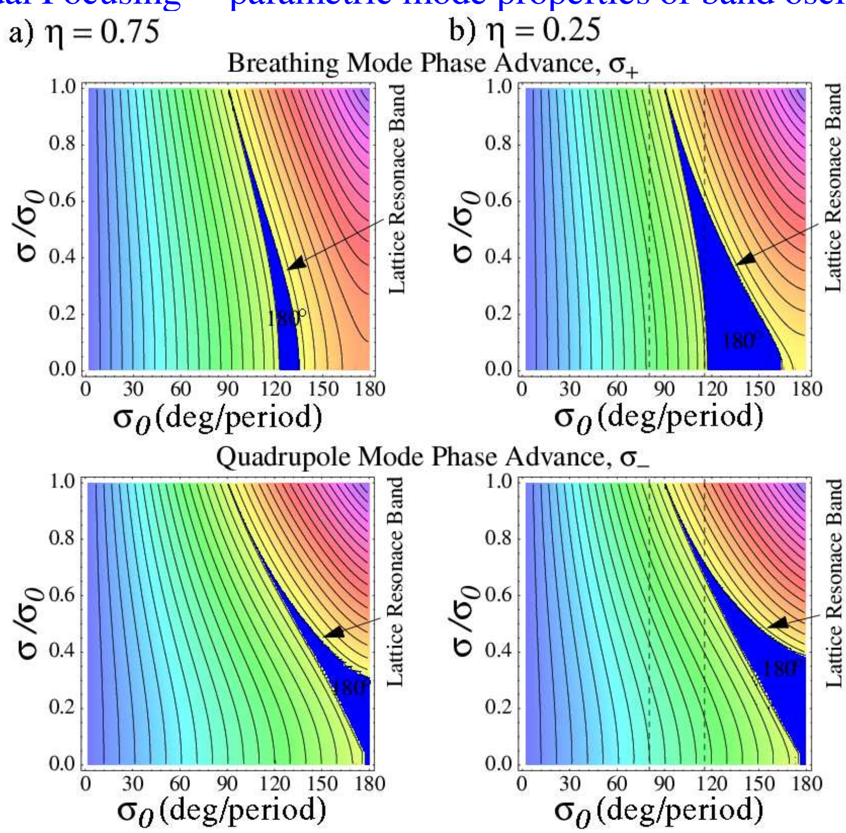

Quadrupole Doublet Focusing – Matched Envelope Solution

FODO and Syncopated Lattices

a) $\sigma_0 = 80°$, $\eta = 0.6949$, and $\alpha = 1/2$

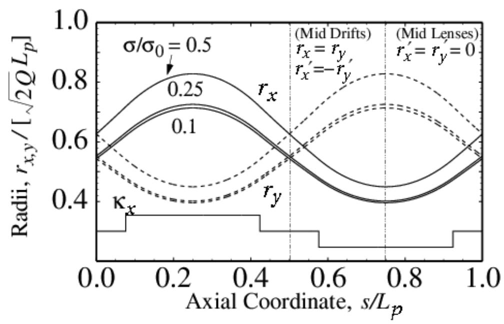

b) $\sigma_0 = 80°$, $\eta = 0.6949$, and $\alpha = 0.1$

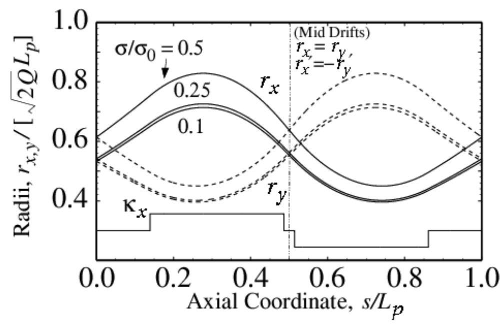

Focusing:

$$\kappa_x(s) = -\kappa_y(s) = \kappa_q(s)$$

$$\kappa_q(s + L_p) = \kappa_q(s)$$

Matched Beam:

$$r_{xm}(s + L_p) = r_{xm}(s)$$
$$r_{ym}(s + L_p) = r_{ym}(s)$$

Using a transfer matrix approach on undepressed single-particle orbits set the strength of the focusing function for specified undepressed particle phase advance:

Quadrupole Focusing:

$$\cos\sigma_0 = \cos\Theta\cosh\Theta + \frac{1-\eta}{\eta}\Theta(\cos\Theta\sinh\Theta - \sin\Theta\cosh\Theta)$$
$$- 2\alpha(1-\alpha)\frac{(1-\eta)^2}{\eta^2}\Theta^2\sin\Theta\sinh\Theta$$

$$\Theta \equiv \frac{\sqrt{|\hat{\kappa}_q|}L_p}{2}$$

Quadrupole Focusing – parametric plots of breathing and quadrupole envelope mode phase advances two values of undepressed phase advance

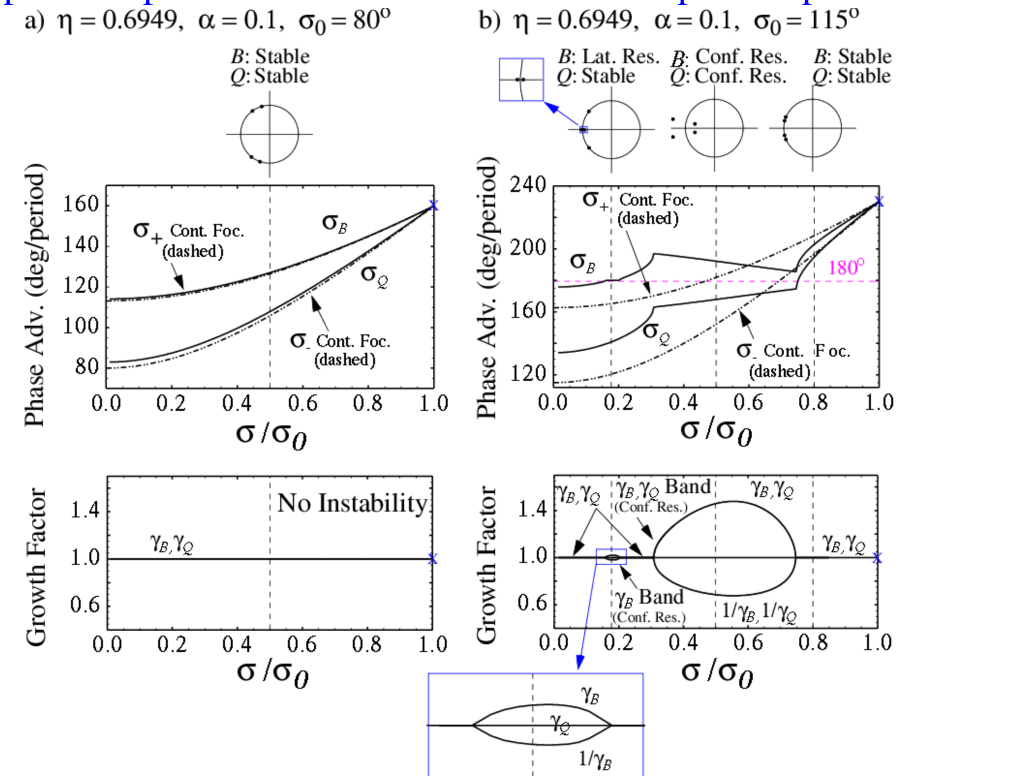

Quadrupole Focusing – mode instability bands vary little/strongly with occupancy for FODO/syncopated lattices

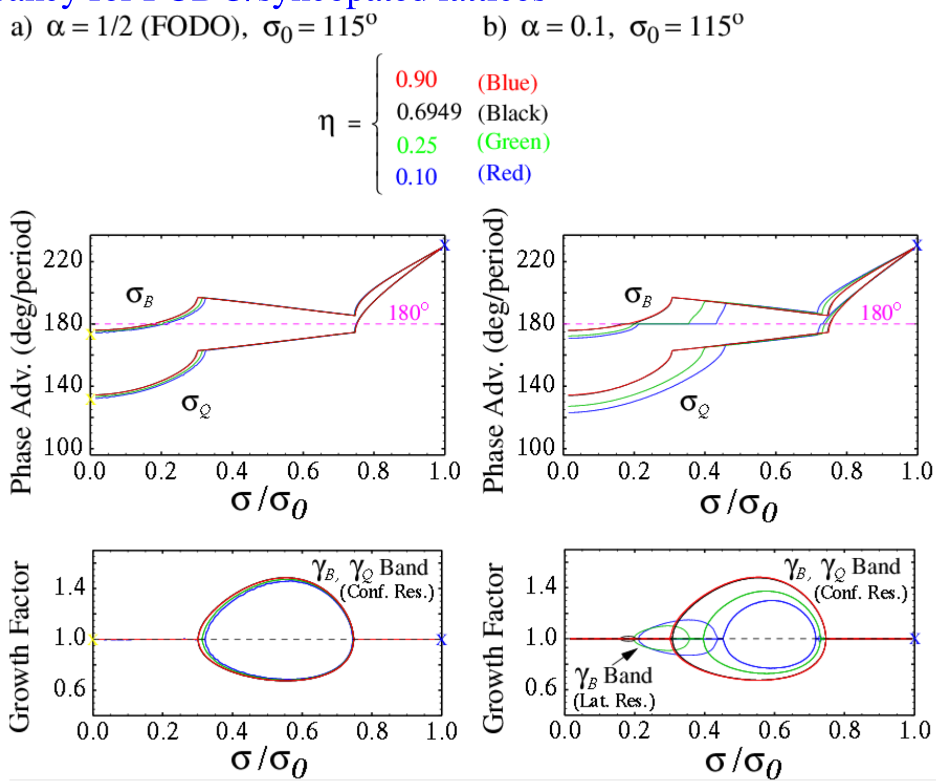

Quadrupole Focusing – broad ranges of parametric instability are found for the breathing and quadrupole bands that must be avoided in machine operation

FODO Lattice
$\eta = 0.6949, \;\; \alpha = 1/2$

Syncopated Lattice
$\eta = 0.6949, \;\; \alpha = 0.1$

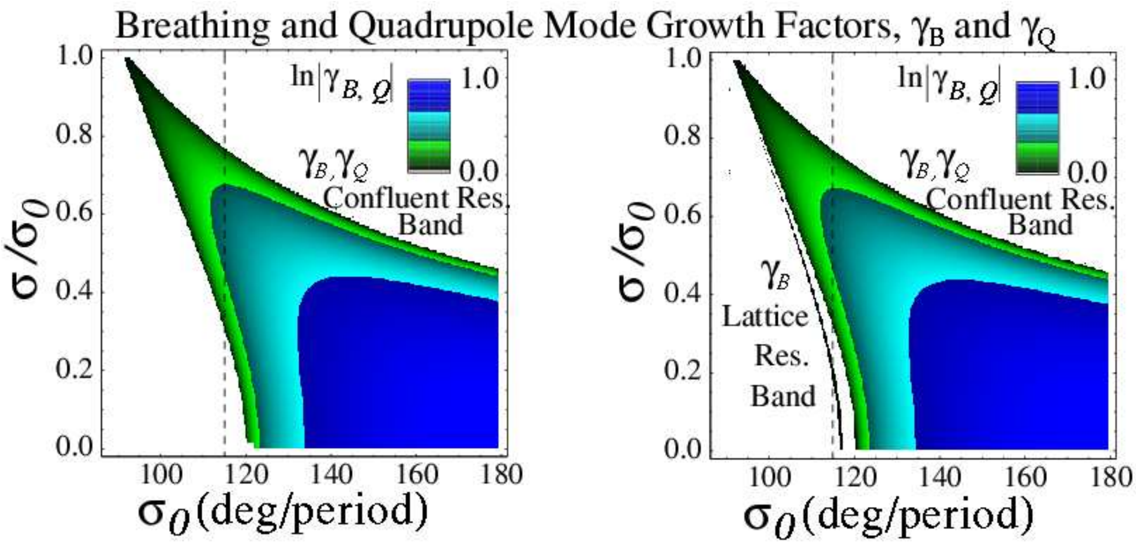

Quadrupole Focusing – parametric mode properties of band oscillations

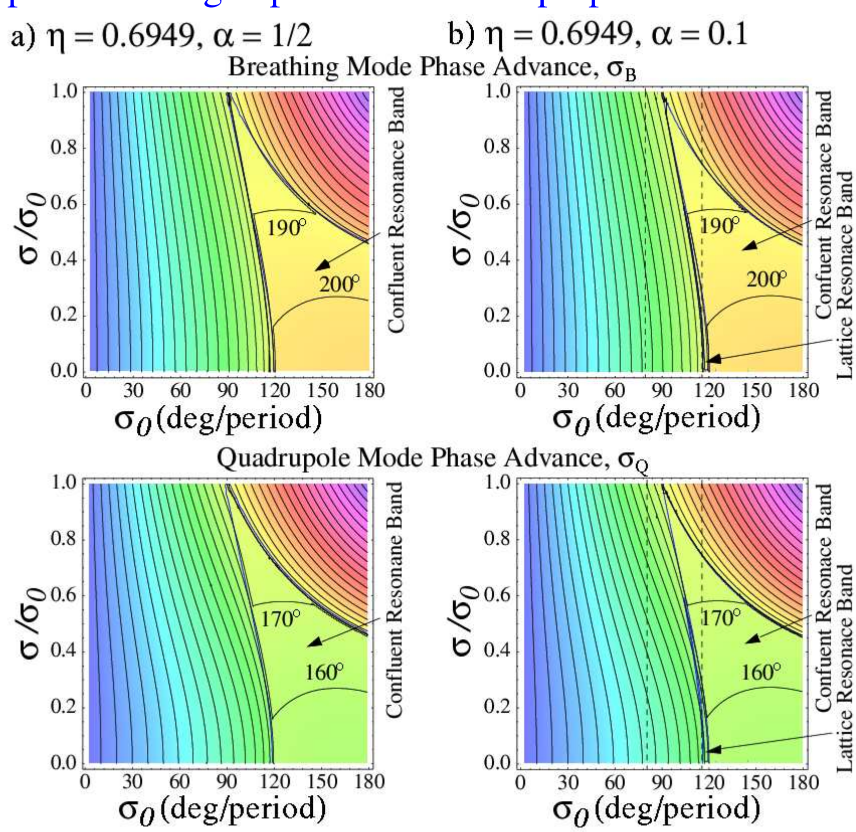

Quadrupole Focusing – mode structure varies strongly with mode phase and the location in the lattice (FODO example)

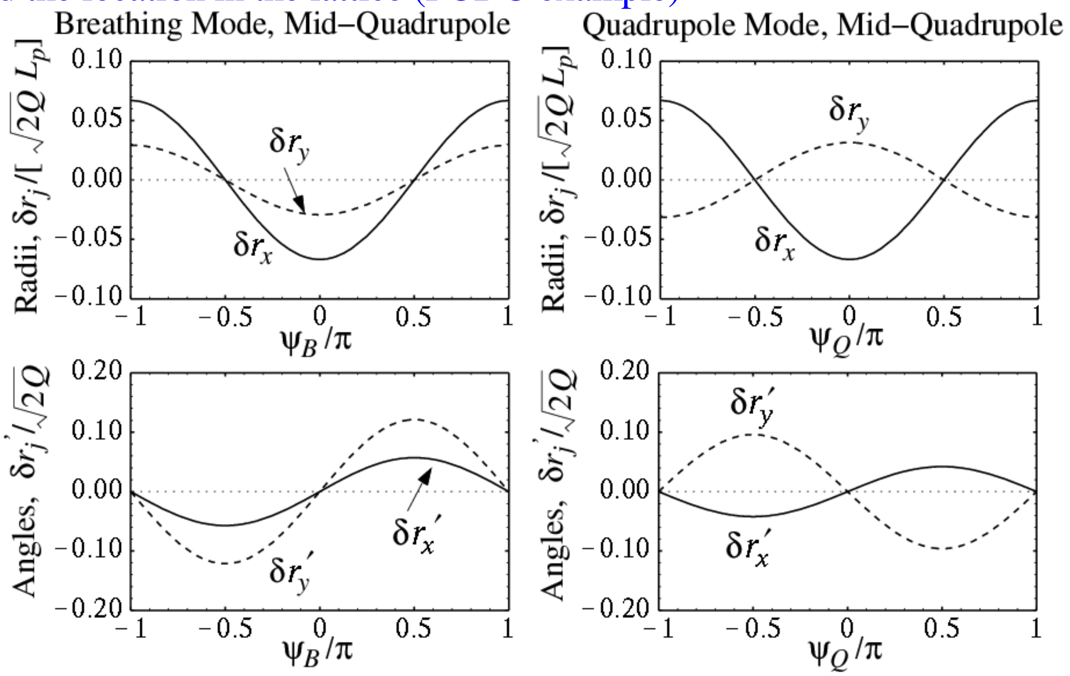

$\delta r_x \neq \delta r_y$	$\delta r_x \neq -\delta r_y$
generally not exact	generally not exact
breathing symmetry	quadrupole symmetry

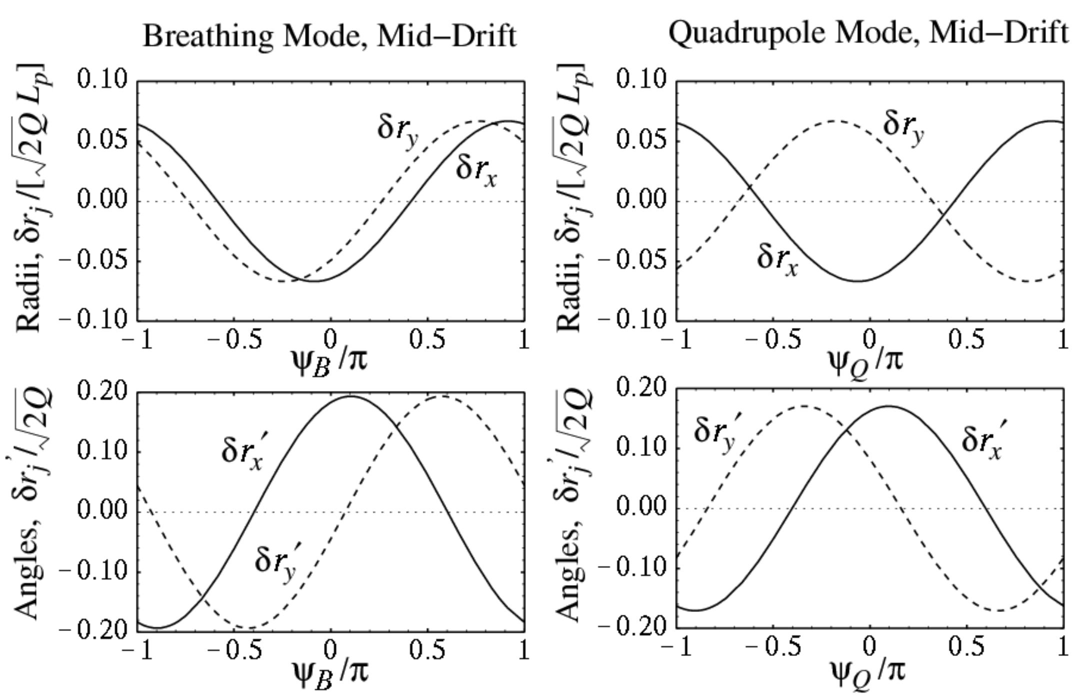

$\delta r_x \neq \delta r_y$	$\delta r_x \neq -\delta r_y$
generally not exact	generally not exact
breathing symmetry	quadrupole symmetry

Summary: Envelope band instabilities and growth rates for periodic solenoidal and quadrupole doublet focusing lattices

Envelope Mode Instability Growth Rates

Solenoid (η = 0.25) Quadrupole FODO (η = 0.70)

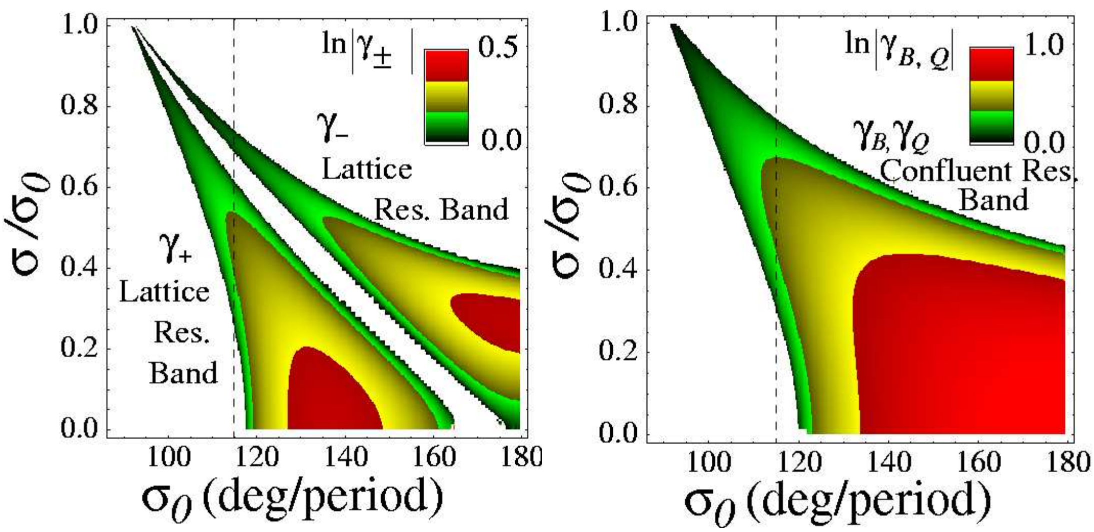

[S.M. Lund and B. Bukh, PRSTAB 024801 (2004)]

S9: Transport Limit Scaling Based on Envelope Models

See Handwritten Notes

S8: Centroid and Envelope Descriptions via 1st Order Coupled Moment Equations

To include in future editions of notes

References: For more information see:

Image charge couplings:

E. P. Lee, E. Close, and L. Smith, Nuc. Inst. And Methods, 1126 (1987)

Seminal work on envelope modes:

J. Struckmeier and M. Reiser, *Theoretical Studies of Envelope Oscillations and Instabilities of Mismatched Intense Charged-Particle Beams in Periodic Focusing Channels*, Part. Accel. **14,** 227 (1984)

M. Reiser, *Theory and Design of Charged Particle Beams* (John Wiley, 1994)

Extensive review on envelope instabilities:

S. M. Lund and B. Bukh, *Stability Properties of the KV Envelope Equations Describing Intense Ion Beam Transport,* PRSTAB **7** 024801 (2004)

KV results:

F. Sacherer, *Transverse Space-Charge Effects in Circular Accelerators*, Univ. of California Berkeley, Ph.D Thesis (1968)

I. Kaphinskij and V. Vladimirskij, in *Proc. Of the Int. Conf. On High Energy Accel. and Instrumentation* (CERN Scientific Info. Service, Geneva, 1959) p. 274

Symmetries and phase-amplitude methods:

A. Dragt, *Lectures on Nonlinear Orbit Dynamics* in *Physics of High Energy Particle Accelerators,* (American Institute of Physics, 1982), AIP Conf. Proc. No. 87, p. 147

E. D. Courant and H. S. Snyder, *Theory of the Alternating-Gradient Synchrotron*, Annals of Physics **3**, 1 (1958)

Analytical analysis of matched envelope solutions and transport scaling:

E. P. Lee, *Precision matched solution of the coupled beam envelope equations for a periodic quadrupole lattice with space-charge*, Phys. Plasmas 9, 4301 (2005).

J.J. Barnard and S.M. Lund
USPAS, June 2006

§9 Transport Limit Scaling Based on the Matched Beam Envelope Equations for Periodic Focusing Channels

The scaling of the maximum beam current, or equivalently, the maximum perveance Q that can be transported at a given energy with a specified focusing technology and lattice is of critical importance in designing optimal transport and acceleration channels. Needed equations can be derived from approximate analytical solutions to the matched beam envelope equations for a given lattice. Alternatively, numerical solutions of the envelope equations can be evaluated. But analytical solutions are preferable to understand scaling and enable rapid evaluation of design tradeoffs.

As a practical matter, equations derived must be applied to regimes where technology is feasible.

- Magnet Field Limits
- Electron breakdown
- Vacuum

⋮

Transport limits are inextricably linked to technology. Moreover, higher order stability constraints etc. must also be respected. Treatments of these topics are beyond the scope of this class. Here we present simplified treatments to highlight issues and methods.

First review an example sketched by J. J. Barnard in the Intro. lectures.

Transport Limits of a Periodic FODO Quadrupole Transport Channel

$$r_{xm}'' + \frac{(\gamma_b\beta_b)'}{(\gamma_b\beta_b)} r_{xm}' + \kappa_x r_{xm} - \frac{2Q}{r_{xm}+r_{ym}} - \frac{\varepsilon_x^2}{r_{xm}^3} = 0$$

$$r_{ym}'' + \frac{(\gamma_b\beta_b)'}{(\gamma_b\beta_b)} r_{ym}' - \kappa_x r_{ym} - \frac{2Q}{r_{xm}+r_{ym}} - \frac{\varepsilon_y^2}{r_{ym}^3} = 0$$

$$r_{xm}(s+L_p) = r_{xm}(s) \quad ; \quad r_{ym}(s+L_p) = r_{ym}(s)$$

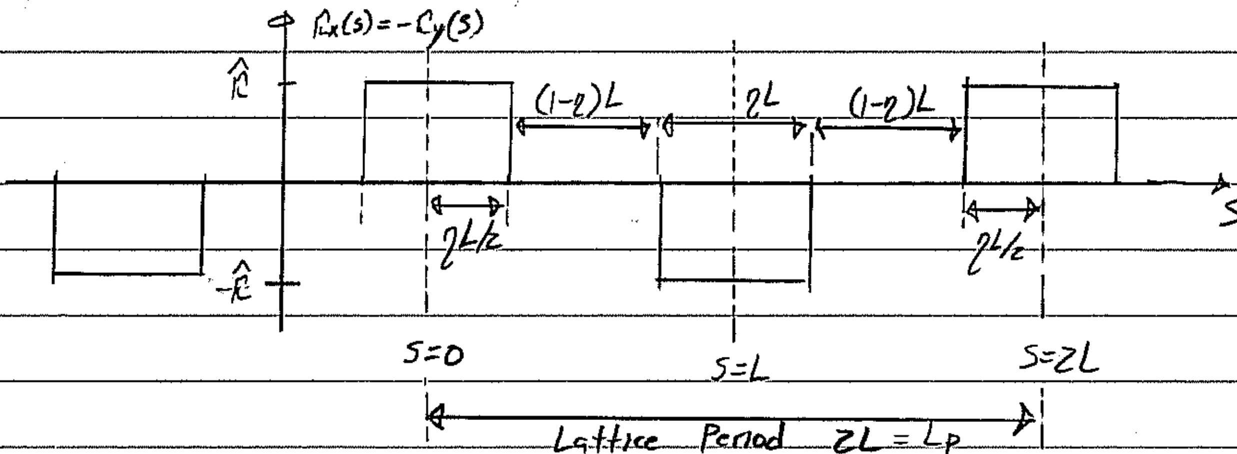

L = Half-Period $\quad L = L_p/2$

η = Quadrupole "occupancy" $\quad 0 < \eta \leq 1$

κ = Focus strength $\quad \kappa = \begin{cases} \dfrac{qE_x'(s)}{m\gamma_b\beta_b^2c^2} \ ; & \text{Electric} \\ \dfrac{qB_y'(s)}{m\gamma_b\beta_b c} \ ; & \text{Magnetic} \end{cases}$

Expand $\kappa_x(s)$ as a Fourier Series:

$$\boxed{\begin{aligned} \kappa_x(s) &= \sum_{n=1}^{\infty} \kappa_n \cos\left(\frac{n\pi s}{L}\right) \\ \kappa_n &= \frac{1}{L}\int_0^{2L} \kappa_x(s)\cos\left(\frac{n\pi s}{L}\right) = \frac{2\hat{\kappa}}{n\pi}\left[1-(-1)^n\right]\sin\left(\frac{n\pi\eta}{2}\right) \end{aligned}}$$

And expand the periodic matched beam envelope by:

$$r_{xm} = r_b\left[1 + \Delta\cos\left(\frac{\pi s}{L}\right)\right] + \sum_{n=2}^{\infty}\Delta_{xn}\cos\left(\frac{n\pi s}{L}\right)$$

$$r_{ym} = r_b\left[1 - \Delta\cos\left(\frac{\pi s}{L}\right)\right] + \sum_{n=2}^{\infty}\Delta_{yn}\cos\left(\frac{n\pi s}{L}\right)$$

r_b = const = avg. beam radius.

$|\Delta|$ = const $\ll 1$

$\Delta_{\substack{x \\ y}n}$ constants with $|\Delta_{\substack{x \\ y}n}| \ll |\Delta|$

Take:

- $(\gamma_b\beta_b)' = 0$ $\Rightarrow$ coasting beam
- $\varepsilon_x = \varepsilon_y = \varepsilon$ $\Rightarrow$ isotropic beam

and insert these expansions in the envelope equations.

Neglect:

- All terms $\mathcal{O}(\Delta^2)$ and higher
- Fast oscillation terms $\sim \cos\left(\frac{n\pi s}{L}\right)$ with $n \geq 2$.

to obtain two independent constraint equations:

Avg (const): $\quad \dfrac{2\Delta\hat{\kappa}}{\pi}\, r_b \sin\left(\dfrac{\pi}{2}\eta\right) - \dfrac{Q}{r_b} - \dfrac{\varepsilon^2}{r_b^3} = 0$

Fundamental $\propto \cos\left(\frac{\pi s}{L}\right)$: $\quad -\Delta\left(\dfrac{\pi}{L}\right)^2 r_b + \dfrac{4\hat{\kappa}\, r_b}{\pi}\sin\left(\dfrac{\pi}{2}\eta\right) + \dfrac{3\Delta\varepsilon^2}{r_b^3} = 0$

These equations can be solved to express the maximum beam edge excursion as

$$\boxed{\mathrm{Max}[r_{xm}] = \mathrm{Max}[r_{ym}] \simeq r_b(1+|\Delta|) = r_b\left\{1 + \frac{4|\hat{\kappa}|L^2}{\pi^3} \frac{\sin\left(\frac{\pi\eta}{2}\right)}{\left(1 - 3\frac{L^2\varepsilon^2}{\pi^2 r_b^4}\right)}\right\}}$$

and the beam Perveance as:

$$\boxed{Q = \frac{2}{\pi^2}\left[\frac{\sin\left(\frac{\pi\eta}{2}\right)}{\left(\frac{\pi\eta}{2}\right)}\right]^2 \frac{\eta^2\hat{\kappa}^2L^2r_b^2}{\left(1 - \frac{3L^2\varepsilon^2}{\pi^2 r_b^4}\right)} - \frac{\varepsilon^2}{r_b^2}}$$

Design Strategy:

1) Choose a lattice period $2L$, quadrupole occupancy η, and clear machine "pipe" radius r_p consistent with focusing technology employed.

2) Choose the largest possible focus strength $\hat{\kappa}$ (quadrupole current or voltage excitation) for beam energy with undepressed particle phase advance:

$$\boxed{\sigma_0 \lesssim 80^\circ/\text{period}, \quad \text{"Tiefenback Limit"}}$$

- Larger phase advances correspond to stronger focus and smaller beam cross-sectional area for given values of Q, ε.

- Weaker phase advance suppresses various particle, envelope, and collective instabilities for reliable transport: [Ref: M.G. Tiefenback, "Space-Charge Limits on the Transport of Ion Beams," UC. Berkeley Ph.d Thesis, 1986 LBL-22465

3) Choose a suitable beam-edge to aperture clearance factor:

$$\boxed{\begin{aligned} r_p &= \text{Max}[r_{xm}] + \Delta_p \\ \Delta_p &= \text{Clearance.} \end{aligned}}$$

to allow for misalignments, limit scraping of halo particles outside the beam core, reduce image charges, gas propagation times from the aperture to the beam, and other nonideal effects.

4) Evaluate choices made using higher-order theory, numerical simulations etc. Iterate choices made to reoptimize when evaluating cost.

Effective application of this formulation requires extensive practical knowledge:

- Nonideal effects: collective instabilities, halo, electron and gas interactions (species contamination), ...
- Technology limits: Voltage breakdown, vacuum, superconducting magnets, ...

In practice, for intense beam transport, the emittance terms $\varepsilon_x, \varepsilon_y$ can often be neglected for the purpose of obtaining simpler scaling relations that are more easily understood.

$$\lim_{\varepsilon_x \to 0} \delta_x = 0$$

$$\lim_{\varepsilon_y \to 0} \delta_y = 0$$

$\Rightarrow$ Full space charge depression

In this limit $Q \to Q_{max}$, the maximum transportable perveance.

For our previous example for FODO quadrupoles, the $\varepsilon \to 0$ limit obtains:

$$\lim_{\varepsilon \to 0} \mathrm{Max}[r_{xm}] = r_b \left\{ 1 + \frac{4|\hat{\kappa}| L^2}{\pi^3} \sin\left(\frac{\pi}{2}\eta\right) \right\}$$

$$\lim_{\varepsilon \to 0} Q = Q_{max} = \frac{2}{\pi^2} \left[\frac{\sin\left(\frac{\pi}{2}\eta\right)^2}{\left(\frac{\pi}{2}\eta\right)} \right] \eta^2 \hat{\kappa}^2 L^2 r_b^2$$

Unfortunately, the method introduced before are inadequate for lattices with lesser degrees of symmetry such as syncopated quadrupole doublet lattices. However, methods introduced by Lee [E. P. Lee, Physics of Plasmas 9, 4301 (2002)], can be applied in this situation and also obtain more accurate results. It is beyond the scope of this class to carry out derivations with these methods, but we summarize results derived.

Quadrupole Doublet Lattice

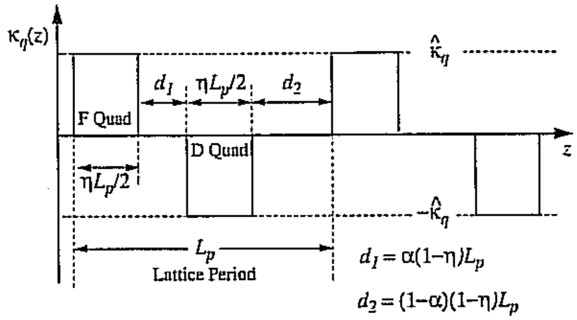

Denote:

Avg Radius: $\bar{r}_m = \int_0^{L_p} \frac{ds}{L_p} r_{xm}(s) = \int_0^{L_p} \frac{ds}{L_p} r_{ym}(s)$

Max Excursion in period: $\mathrm{Max}[r_m] \equiv \mathrm{Max}[r_{xm}, r_{ym}]$

Phase Advance

$$\cos\sigma_0 = 1 - \frac{(\eta\widehat{\kappa_q}L_p^2)^2}{32}\left[\left(1-\frac{2}{3}\eta\right) - 4\left(\alpha-\frac{1}{2}\right)^2(1-\eta)^2\right].$$

For $\sigma_0 = 80^\circ$

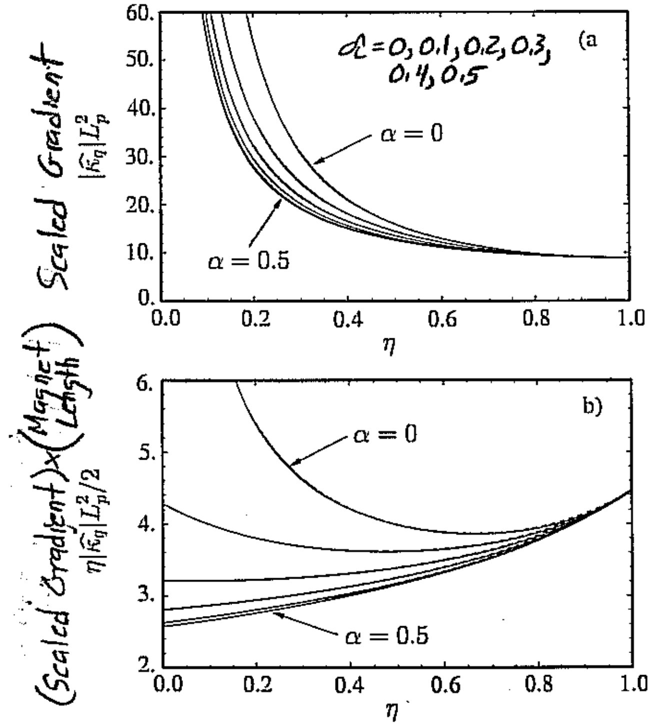

Envelope Flutter

$$\frac{\mathrm{Max}[r_m]}{\overline{r_m}} - 1 = \frac{(1-\cos\sigma_0)^{1/2}(1-\eta/2)[1-4(\alpha-1/2)^2(1-\eta)^2]}{2^{3/2}\left[(1-2\eta/3)-4(\alpha-1/2)^2(1-\eta)^2\right]^{1/2}}.$$

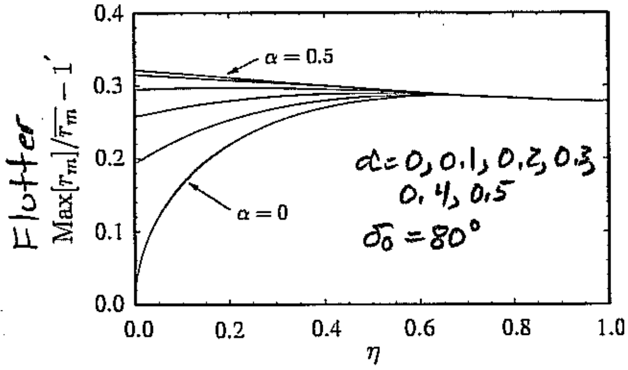

Relations Connecting Max Transportable Perveance Qmax and Lattice Parameters

$$Q_{\max} = \frac{(1-\cos\sigma_0)^{1/2}}{2^{3/2}} \frac{\eta[(1-2\eta/3) - 4(\alpha-1/2)^2(1-\eta)^2]^{1/2}}{(\mathrm{Max}[r_m]/\overline{r_m})^2} |\widehat{\kappa_q}| \, \mathrm{Max}[r_m]^2$$
$$= \frac{(1-\cos\sigma_0)^{1/2}}{2^{3/2}} \frac{\eta[(1-2\eta/3) - 4(\alpha-1/2)^2(1-\eta)^2]^{1/2}}{\left\{1 + \frac{(1-\cos\sigma_0)^{1/2}(1-\eta/2)[1-4(\alpha-1/2)^2(1-\eta)^2]}{2^{3/2}[(1-2\eta/3)-4(\alpha-1/2)^2(1-\eta)^2]^{1/2}}\right\}^2} |\widehat{\kappa_q}| \, \mathrm{Max}[r_m]^2.$$

$$\frac{\mathrm{Max}[r_m]}{L_p} = \sqrt{\frac{Q_{\max}}{2(1-\cos\sigma_0)}} \left(\frac{\mathrm{Max}[r_m]}{\overline{r_m}}\right)$$
$$= \sqrt{\frac{Q_{\max}}{2(1-\cos\sigma_0)}} \left\{1 + \frac{(1-\cos\sigma_0)^{1/2}(1-\eta/2)[1-4(\alpha-1/2)^2(1-\eta)^2]}{2^{3/2}\,[(1-2\eta/3)-4(\alpha-1/2)^2(1-\eta)^2]^{1/2}}\right\},$$

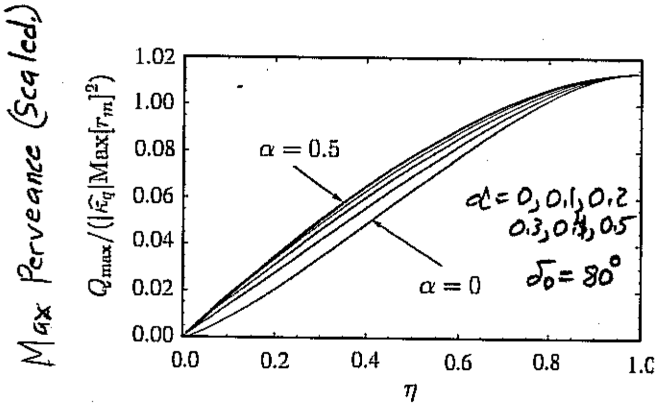

Derivation and aplication of scaling relations can be complicated. They are often applied in systems codes to generate plots that can be interpreted more readily.